Noise-induced symmetry breaking far from equilibrium and the emergence of biological homochirality

Farshid Jafarpour*
Department of Physics and Astronomy, Purdue University, 525 Northwestern Avenue, West Lafayette, Indiana 47907, USA

Tommaso Biancalani
Physics of Living Systems, Department of Physics, Massachusetts Institute of Technology, Cambridge, Massachusetts 02139, USA

Nigel Goldenfeld
Department of Physics, University of Illinois at Urbana-Champaign, Loomis Laboratory of Physics, 1110 West Green Street, Urbana, Illinois 61801, USA
and Carl R. Woese Institute for Genomic Biology, University of Illinois at Urbana-Champaign, 1206 West Gregory Drive, Urbana, Illinois 61801, USA
(Received 13 November 2016; published 10 March 2017)

The origin of homochirality, the observed single-handedness of biological amino acids and sugars, has long been attributed to autocatalysis, a frequently assumed precursor for early life self-replication. However, the stability of homochiral states in deterministic autocatalytic systems relies on cross-inhibition of the two chiral states, an unlikely scenario for early life self-replicators. Here we present a theory for a stochastic individual-level model of autocatalytic prebiotic self-replicators that are maintained out of thermal equilibrium. Without chiral inhibition, the racemic state is the global attractor of the deterministic dynamics, but intrinsic multiplicative noise stabilizes the homochiral states. Moreover, we show that this noise-induced bistability is robust with respect to diffusion of molecules of opposite chirality, and systems of diffusively coupled autocatalytic chemical reactions synchronize their final homochiral states when the self-replication is the dominant production mechanism for the chiral molecules. We conclude that nonequilibrium autocatalysis is a viable mechanism for homochirality, without imposing additional nonlinearities such as chiral inhibition.

DOI: 10.1103/PhysRevE.95.032407

Homochirality, the single-handedness of all biological amino acids and sugars, is one of two major universal features of life on Earth. The other is the canonical genetic code. Their universality transcends all categories of life, up to and including the three domains, and thus requires an explanation that transcends the idiosyncrasies of individual organisms and particular environments. The only universal process common to all life is, of course, evolution, and so it is natural to seek an explanation for biological homochirality in these terms, just as has been done to account for the universality and error-minimization aspects of the genetic code [1]. This paper is just such an attempt, using the simplest and most general commonly accepted attributes of living systems.

The origin of biological homochirality has been one of the most debated topics since its discovery by Louis Pasteur in 1848 [2]. There are those who argue that homochirality must have preceded the first chemical systems undergoing Darwinian evolution, and there are those who believe homochirality is a consequence of life, but not a prerequisite [3]. There are even those who argue that homochirality is a consequence of underlying asymmetries from the laws of physics, invoking complicated astrophysical scenarios for the origin of chiral organic molecules [4] or even the violation of parity from the weak interactions [5,6]! In fact, explanations that are based on physical asymmetries can only predict an enantiomeric excess of one handedness over another, and not the 100% effect observed in nature [7].

The most influential class of theories for biological homochirality rest on an idea of F.C. Frank's, in which there is a kinetic instability of a racemic (50% right handed and 50% left handed) mixture of chiral molecules produced by certain autocatalytic reactions [8]. The theory additionally invokes a mutually antagonistic relationship between the two enantiomers of the chiral molecule, known as "chiral inhibition", and has led to a large literature of specific realizations for Frank's spontaneous symmetry-breaking mechanism [8–15]. Although autocatalysis is an expected prerequisite for early life self-replicators, the mutually antagonistic relationship between the two chiral molecules does not seem to be biologically necessary [16] and might in principle depend on when we place the origin of homochirality with respect to the origin of life [17].

When this mutual antagonistic relationship is replaced by linear growth and decay reactions, the racemic state becomes the global attractor of the deterministic dynamics, rather than a repellor. In this case, the deterministic analysis of the model indicates that even if the system is initialized in a homochiral state, it ends up with a final racemic state. However, when the effect of chemical number fluctuations from self-replication is taken into account, the system can transition to homochirality when the autocatalysis is the dominant mechanism for the production of the chiral molecules [17].

The purpose of this paper is to present a detailed analysis of this noise-induced symmetry breaking in a nonequilibrium autocatalytic model of self-replicating chiral molecules without chiral inhibition along with its spatial extension. This paper is an expansion and elaboration of our paper [17], which originally reported the emergence of homochirality in an

*Corresponding author: fjafarpo@purdue.edu

autocatalytic model without chiral inhibition by incorporating the effect of chemical number fluctuation (i.e., multiplicative noise).

This paper is organized as follows. We start with an introduction to the basic concepts of chirality of molecules and biological homochirality followed by an account of Frank's spontaneous symmetry-breaking model of homochirality [8] in Sec. I. This sets the stage for Sec. II, where we replace the reaction modeling the mutual antagonistic relationship in Frank's model by linear decay and growth reactions and show that even though the racemic solution is the global attractor of the deterministic dynamics, when the intrinsic stochasticity of the self-replication process is taken into the account, the system transitions to homochirality. This transition takes place when the efficiency of self-replication exceeds a threshold. The relationship between the transition to homochirality in this model and the emergence of early life is discussed in Sec. II C. In Sec. II D, we discuss the nonequilibrium aspects of our model and the principle of detailed balance. In particular, we point out that life fundamentally breaks microscopic reversibility, so that living processes must violate the principle of detailed balance, reflecting the requirement for an external energy source to power the system, such as the Sun or radioactive heating. The stochastic theory for the emergence of biological homochirality then relies on three key attributes of life: autocatalysis, the driving far from equilibrium, and the increasing efficiency of autocatalytic production as life becomes more efficient and (presumably) complex. This stochastic mechanism for homochirality depends on intrinsic noise, and thus it is important to determine how robust it is with respect to spatial inhomogeneities. In Sec. III, first, we show that when a well-mixed system described by this model is perturbed by diffusion of chiral molecules of perhaps opposite chirality from neighboring well-mixed systems, the system maintains its homochirality. Then we show that in a continuous one-dimensional model, the reactions at different points in space synchronize their final homochiral state, showing that this noise-induced mechanism for the origin of homochirality is robust with respect to the spatial extension. Potential implications of this model and future directions are discussed in Sec. IV.

I. INTRODUCTION TO HOMOCHIRALITY

In this section, we will give an introduction to the basic concepts related to chirality of organic molecules and biological homochirality. A review of spontaneous and explicit symmetry-breaking theories of homochirality is given in Sec. I B. The main focus of this work is on spontaneous symmetry-breaking mechanisms. All of the previous spontaneous symmetry-breaking models of homochirality have the same basic mechanism [15] as Frank's model [8], which is reviewed in Sec. I C. Frank has shown that in a population of self-replicating (autocatalytic) chiral molecules that are mutually antagonistic, the racemic solution is unstable. While autocatalysis is expected in a model of prebiotic chemistry, the mutual antagonistic relationship may not have an obvious biological justification, nor may it be a generic feature of early life. Thus it is important to understand whether chiral inhibition is a necessary or merely a sufficient condition for chiral symmetry breaking.

A. Molecular chirality

In 1848 Pasteur discovered that the sodium ammonium salt of synthetic tartaric acid (known at the time as racemic[1] acid) produces two distinct types of crystals known as "+" and "−" forms, which are mirror images of one another. Pasteur showed that if we shine linearly polarized light through solutions made by each one of these two types of crystals, they rotate the angle of polarization of light in opposite directions. He concluded that the racemic acid was made of two kinds of molecules with opposite optical activity, and the asymmetry of the crystals was related to an asymmetry at the molecular level [2]. A clear explanation did not emerge until 1874, when van't Hoff and Le Bel independently discovered that organic molecules with a carbon atom connecting to four different groups are not mirror symmetric, and as a result, the groups can be placed around the carbon atom in two distinct ways: left-handed and right-handed order, two configurations that are mirror images of one another [18,19]. Molecules that are not superimposable on their mirror image are called chiral (Greek for hand), and the atom surrounded by four different groups is known as the chiral center of the molecule.

There are at least three different, but arbitrary, conventions to determine which one of the two optical isomers (also known as *enantiomers*) should be called left-handed, and which one should be called right-handed:

(1) The (+) and (−) classification based on the optical activity explained above is important for historical reasons but is not very useful for our purpose, as there is no way to determine the optical activity just by looking at the structure of the molecule. Moreover, the optical activity of the chiral solutions could also depend on the properties of the solvent.

(2) More commonly used in chemistry is the *R*/*S* (referring to *Rectus* and *Sinister,* Latin for right-handed and left-handed, respectively) nomenclature, where the ordering of the groups on the chiral centers is chosen based on the atomic numbers, and can be easily determined by looking at the three-dimensional structure of the molecule. However, atomic number is not always the most biologically relevant criterion, and as it turns out, the *R*/*S* classification does not consistently maintain the ordering of the functional groups across, e.g., all amino acids.

(3) The D-L (named after *Dexter* and *Laevus,* Latin for right and left, respectively) convention (also known as the Fisher-Rosanoff convention) is chosen for a molecule if it can be theoretically derived from *R*/*S*-glyceraldehyde without changing the configuration of the chiral center [20]. This seemingly arbitrary convention happens to be the one that

[1]The word "racemic" derives from the Latin for "bunch of grapes," and at the time, it was used to refer to crystals of synthetic tartaric acid, because tartaric acid is naturally found in grapes. However, the tartaric acid found in grapes does not produce the two distinct crystals, since it is produced biologically and is homochiral. The word racemic is nowadays used to mean a 50-50 mixture of two chiral molecules, which could be misleading knowing the etymology of the word.

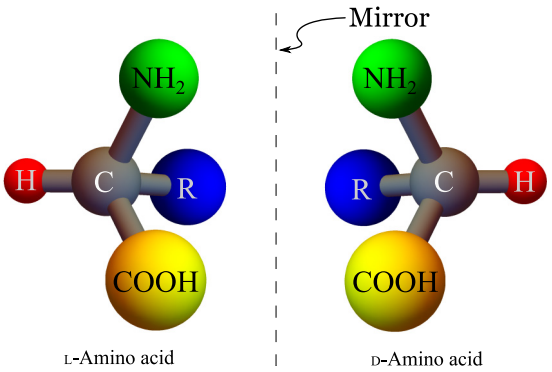

FIG. 1. Ball-and-stick model of a generic α-amino acid and its mirror image. α-amino acids are organic compounds with a chiral carbon connected to an amino group ($-NH_2$), a carboxylic acid group ($-COOH$), a hydrogen atom ($-H$), and a side chain ($-R$) that varies depending on the particular amino acid. The L or D chirality of amino acids is determined by the CORN rule: an amino acid is L-chiral (D-chiral) if by wrapping your left hand (right hand) fingers around the direction of CORN ($-CO$, $-R$, and $-N$ groups in order) your thumb points toward the direction of the hydrogen atom.

keeps the order of similar functional groups in biological molecules consistent and makes it possible to compare the chirality of different molecules with similar groups such as different amino acids (see Fig. 1).

It is important to note that there is no fixed relation between the three arbitrary conventions, since a right-handed molecule in one convention can be left-handed in the other.

Parity is a symmetry of the laws of physics (weakly broken at small length and time scales by the weak interaction). In particular, two enantiomers of a chiral molecule have identical physical, chemical, and thermodynamical properties. Therefore, chemical reactions producing chiral molecules from achiral molecules, by symmetry, are expected to produce solutions of 50% right-handed and 50% left-handed molecules. Such solutions are called racemic. In contrast, a solution of all left-handed or all right-handed molecules is called homochiral or enantiopure.

B. Biological homochirality: A symmetry-breaking problem

Amino acids are building blocks of proteins, and their chirality plays an important role in the structure and the function of proteins in living cells. Sugars are often used as a storage for chemical energy in biological systems, but perhaps more importantly, sugars play a key role in the structure of RNA and DNA molecules. The famous double helix structure of DNA is a result of the chirality of the sugar molecules in its backbone. Despite the diversity of proteins and their functions virtually all chiral biological amino acids[2] are L-chiral,[3] while all sugars are D-chiral.

Homochirality is particularly surprising, in light of the fact that all the physical, chemical, and thermodynamical properties of the two enantiomers of a chiral molecule are identical. This is due to the symmetry of laws of electromagnetism under reflection. When life was emerging on the planet, chiral molecules were formed from simpler achiral molecules that existed in the early atmosphere and the ocean. Since the initial state was symmetric (solution of achiral molecules) and the laws of physics are symmetric, one would expect a symmetric final state, that is, a biosphere made of a racemic solution of chiral molecules. A phenomenon in which the initial state and the corresponding laws of physics are symmetric with respect to a particular transformation, but the final state of the system violates that symmetry, is called a symmetry breaking. There are two resolutions to symmetry-breaking problems: first, explicit symmetry breaking, when the laws of physics are only approximately symmetric, or there is an asymmetric perturbation to the system. Second, in contrast, spontaneous symmetry breaking happens when the governing laws are perfectly symmetric, and as a result, the symmetric state is a final solution, but it may be an unstable solution. In this case, even the slightest perturbation to the system moves the system away from the symmetric state.

There have been some attempts to explain homochirality through explicit symmetry-breaking mechanisms. For example, if life was formed from chiral organic molecules that were produced under a steady radiation of circularly polarized light, the asymmetric interaction of different enantiomers of chiral molecules with the light over hundreds of millions of years could lead to a significant enantiomeric excess [4]. These theories are partly motivated by reports of observation of slight L-enantiomeric excess of some of amino acids found in the Murchison meteorite [7,24,25]. Another example relates to the parity violation of the weak interaction. Unlike electromagnetic interactions, the weak interaction violates mirror symmetry [26,27]. Even though weak interactions have a negligible effect at molecular scales, it has been argued that it can cause an asymmetry affecting the rate of production of two enantiomers in a manner that over billions of years could lead to an observable level of enantiomeric imbalance [5,6].

A common weakness of explicit symmetry-breaking mechanisms is that the homochirality achieved is only partial: These mechanisms lead to an imbalance between the concentrations of the two enantimeres but do not result in complete homochirality. As a result, there is a common misunderstanding in the homochirality literature that the origin of homochirality requires two steps: (1) an explicit symmetry-breaking mechanism to break the symmetry in the initial condition, followed by (2) a mechanism to amplify the initial asymmetry. We believe it is important to clarify this point for the nonphysicist audience: If there is a mechanism amplifying the initial asymmetry for arbitrary small asymmetries, then the symmetric solution is

[2]Of the 23 proteinogenic amino acids found in life, glycine is the only achiral amino acid.

[3]Some D-amino acids do appear in biological system (e.g., D-aspartate is a regulator of adult neurogenesis [21]) and are generated by enzymes that are specialized in the inversion of the stereochemistry (of the corresponding L-amino acids) known as *racemases* and *epimerases*. These amino acids cannot participate in protein structures through ribosomal synthesis but can take part in structure of peptides (e.g., D-phenylalanine in the antibiotic tyrocidine [22]) through either posttranslational conversion of L- to D-amino acids or the activity of nonribosomal peptide synthetases. For a review of the role of D-amino acids, see, for example, Ref. [23]

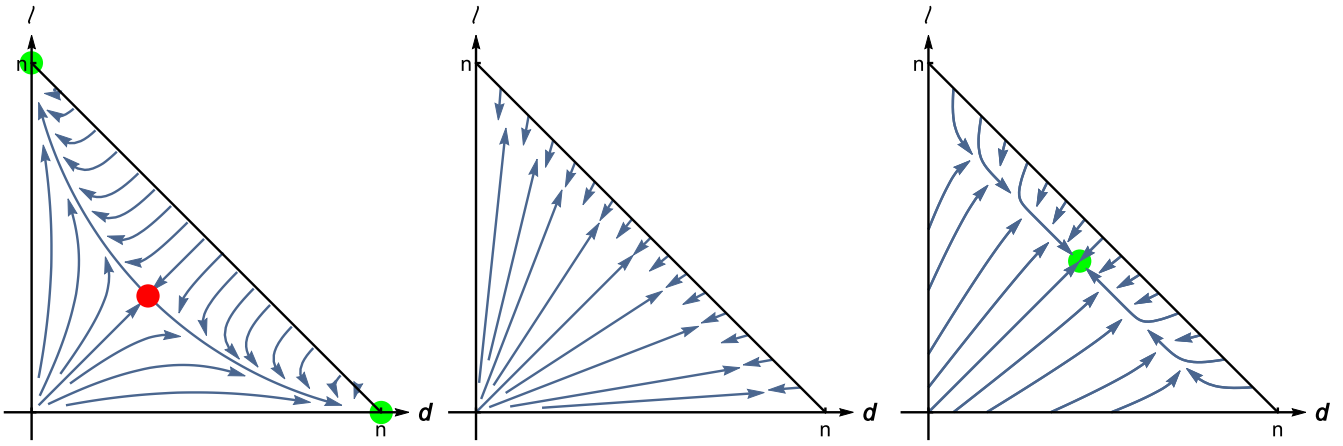

(a) $A + \text{D} \to 2\text{D}$, $A + \text{L} \to 2\text{L}$, $\text{D} + \text{L} \to 2A$ (b) $A + \text{D} \to 2\text{D}$, $A + \text{L} \to 2\text{L}$, $\text{D} \to A$, $\text{L} \to A$ (c) $A + \text{D} \to 2\text{D}$, $A + \text{L} \to 2\text{L}$, $\text{D} \rightleftharpoons A$, $\text{L} \rightleftharpoons A$

FIG. 2. (a) Phase portrait of Frank's model: the racemic state is an unstable fixed point (red dot), while the homochiral states are stable fixed points (green dots). (b) If chiral inhibition is replaced by linear decay reaction, the ratio of D and L molecules stays constant. (c) Adding even the slightest amount of nonautocatalytic production of D and L molecules makes the racemic state (green dot) the global attractor of the dynamics.

unstable, and over time the system decays to one of the two homochiral states, even with a symmetric initial condition; this is spontaneous symmetry breaking.

The first model of spontaneous symmetry breaking for homochirality was proposed by Frank in 1953 [8]. There have been many other models of homochirality since Frank's model, but the underlying mechanism for spontaneous symmetry breaking in all of these models is the same as the mechanism by Frank [15]. Frank's model is reviewed in detail in Sec. I C.

C. Frank's model of homochirality

Frank introduced a model in which the D and L enantiomers of a chiral molecule are autocatalytically produced from an achiral molecule A in reactions

$$A + \text{D} \xrightarrow{k_a} 2\text{D}, \quad A + \text{L} \xrightarrow{k_a} 2\text{L}, \tag{1}$$

and are consumed in a chiral inhibition reaction:[4]

$$\text{D} + \text{L} \xrightarrow{k_i} 2A. \tag{2}$$

The state of this system can be described by the chiral order parameter ω defined as

$$\omega = \frac{[\text{D}] - [\text{L}]}{[\text{D}] + [\text{L}]}, \tag{3}$$

where [D] and [L] are the concentrations of D and L. The order parameter ω is zero at the racemic state, and ± 1 at the homochiral states. In order to determine the time evolution of the order parameter ω, we can use the law of mass action to set the rates of reactions (1) and (2) proportional to the products of the concentrations of the corresponding reactants. The result is the following set of mean field equations for the rate of change of concentrations of A, D, and L:

$$\begin{aligned} \frac{d[A]}{dt} &= 2k_i\,[\text{D}]\,[\text{L}] - k_a\,[A]\,([\text{D}] + [\text{L}]), \\ \frac{d[\text{D}]}{dt} &= k_a\,[A]\,[\text{D}] - k_i\,[\text{L}]\,[\text{D}], \\ \frac{d[\text{L}]}{dt} &= k_a\,[A]\,[\text{L}] - k_i\,[\text{D}]\,[\text{L}]. \end{aligned} \tag{4}$$

The rate of change of ω can be derived from the chain rule, resulting in the mean field equation of motion:

$$\frac{d\omega}{dt} = \frac{1}{2}k_i([\text{D}] + [\text{L}])\omega(1 - \omega^2). \tag{5}$$

Equation (5) has three deterministic fixed points: the racemic state, $\omega = 0$, is an unstable fixed point, and the two homochiral states, $\omega = \pm 1$, are stable fixed points. Starting from almost everywhere in the D-L plane, the system converges to one of the homochiral fixed points [Fig. 2(a)].

In the context of biological homochirality, extensions of Frank's idea have essentially taken two directions. On the one hand, the discovery of a synthetic chemical system of amino alcohols that amplifies an initial excess of one of the chiral states [9] has motivated several autocatalysis-based models (see Ref. [15] and references therein). On the other hand, ribozyme-driven catalyst experiments [28] have inspired theories based on polymerization and chiral inhibition that minimize [10,14,29] or do not include at all [12,30] autocatalysis. Further extensions accounting for both intrinsic noise [15,31] and diffusion [32–35] build further upon Frank's work.

[4] In the original model by Frank, the concentration of the molecules A was kept constant to reduce the degrees of freedom by one, and the chiral inhibition was introduced by the reaction $\text{D} + \text{L} \to \varnothing$. This model leads to indefinite growth of D or L molecules and does not have a well-defined steady state. To resolve this problem, we let the concentration of A molecules be variable and replaced this reaction by $\text{D} + \text{L} \to 2A$, which conserves the total number of molecules. This conservation law reduces the number of degrees of freedom by one again. The mechanism to homochirality in the modified model is the same as the original model by Frank, since the order parameter in both models obeys Eq. (6).

From our perspective, the experimental finding that is most interesting is that chiral inhibition is not a necessary part of autocatalytic reaction schemes. A recent important experimental realization of RNA replication using a novel ribozyme shows such efficient autocatalytic behavior that chiral inhibition does not arise [16]. Thus it becomes critical to ask whether homochirality can arise in the absence of chiral inhibition. As we will see, the answer is yes: chiral inhibition is not a necessary condition for symmetry breaking, although the mechanism is quite different from that envisioned by Frank.

Regardless of the specific model details, all these models share the three-fixed-points paradigm of Frank's model, namely that the time evolution of the chiral order parameter ω is given by a deterministic equation of the form [15]

$$\frac{d\omega}{dt} = f(t)\,\omega(1-\omega^2), \tag{6}$$

where the function $f(t)$ is model-dependent. The sole exception to this three-fixed-points model in a variation of Frank's model is the work of Lente [36], where purely stochastic chiral symmetry breaking occurs, although chiral symmetry breaking is only partial, with $\omega \neq 0$ but $|\omega| < 1$. In all models obeying Eq. (6), the homochiral states arise from a nonlinearity which is not a property of simple autocatalysis, but, for instance, in the original Frank's model, is due to chiral inhibition. To clarify this, one can repeat the analysis of the rate equations for a variation of Frank's model in which the chiral inhibition reaction (2) is broken down into two independent linear decay reactions

$$\mathrm{D} \xrightarrow{k_d} A, \quad \mathrm{L} \xrightarrow{k_d} A. \tag{7}$$

Figure 2(b) shows that in this modified model, the homochiraity is lost, and the ratio of D and L molecules stays constant over time. The situation is even worse: if the reactions (7) are even slightly reversible,

$$\mathrm{D} \underset{k_n}{\overset{k_d}{\rightleftharpoons}} A, \quad \mathrm{L} \underset{k_n}{\overset{k_d}{\rightleftharpoons}} A, \tag{8}$$

the racemic solution becomes the global attractor of the deterministic dynamics [see Fig. 2(c)]. Even starting from a homochiral state, such a system eventually converges to a racemic solution. This structural instability of the chiral inhibition terms in the equation is unphysical, because these small changes to the reaction scheme should not have a qualitatively large impact on the outcome.

In Sec. II, we will show that despite the fact that the stability analysis of rate equations indicates that the modified Frank's model without chiral inhibition approaches a racemic steady state, when the intrinsic noise from the autocatalytic reactions is taken into account, the system can nevertheless transition to homochirality under certain conditions.

II. NOISE-INDUCED ORIGIN OF HOMOCHIRALITY IN PREBIOTIC SELF-REPLICATORS

In this section, we will show that efficient early-life self-replicators can drive the emergence of universal homochirality, through a stochastic treatment of Frank's model *without* requiring nonlinearities such as chiral inhibition. In our stochastic treatment, the homochiral states arise not as fixed points of deterministic dynamics, but instead are states where the effects of chemical number fluctuations (i.e., the multiplicative noise [37]) are minimized. The mathematical mechanism proposed here [38–41] is intrinsically different from that of the class of models summarized by Eq. (6). We conclude that autocatalysis alone can in principle account for universal homochirality in biological systems far from equilibrium, when autocatalysis is the strongly dominant mechanism for the production of chiral molecules.

To be self-contained, we now clarify in what sense chemical reactions are stochastic and when the stochasticity matters. In reaction kinetics, the rate of reactions is usually calculated using the law of mass action. The law of mass action states that the rate of a reaction is proportional to the product of the concentrations of its reactants, and the proportionality constant is defined as the reaction rate. An intuitive explanation of this law is as follows: A chemical reaction takes place when its reactants collide with enough energy to overcome the activation energy of the reaction. The probability of the collision of these reactants is proportional to the product of their concentration, and therefore, the expected value of the number of such collisions per unit time is also proportional to the product of the concentrations of the reactants. This is the law of mass action, and it is an intrinsically mean field approximation.

Near equilibrium, a system of a large number of interacting chemicals follows Boltzmann statistics and can be approximated by its expected value. This approximation is possible because the distribution of various quantities converge to narrow Gaussian distributions around their mean. This is the reason that, in calculating rates of reactions, the expected value of number of collisions is used instead of the actual probability distribution of the number of collisions per unit time.

However, this property is not generalizable to systems that are maintained far from equilibrium. For such systems, instead of using the law of mass action as the expected value of the number of reactions per unit time, it is more appropriate to interpret the law of mass action as the probability per unit time of occurrence of a chemical reaction. Also, instead of the rate equations for the rate of change of the expected value of the concentrations of the reactants and the products, we can write the *master equation* for the rate of change of the probability of the system having given concentrations of reactants and products. A step by step treatment of the master equation is given in Sec. II B. An intuitive explanation of the mechanism for the symmetry breaking and its relationship with the origin of life follows in Sec. II C.

Our proposed reactions [reactions (9)] are chosen as an effective minimal model in which the transition to homochirality via a noise-induced symmetry breaking in the absence of chiral inhibition can be observed. Of course, the actual set of reactions that took place during the emergence of life leading to the symmetry breaking may involve more chemical species and more intermediate steps. In particular, the steady state of our reaction set will be a nonequilibrium steady state implying that self-replication process has to be driven by an external source of energy. This could mean that self-replication may be coupled to other set of reactions, in the same way that some energy-consuming reactions in biological cells are driven by ATP hydrolysis. A more detailed analysis of the

thermodynamical aspects of our model and other variations are discussed in Sec. II D.

A. Description of the stochastic model

Motivated in part by the experimental demonstration of autocatalysis without chiral inhibition [16], we propose the reaction scheme below, which is equivalent to a modification of a model by Lente [36] with the additional process representing the recycling of enantiomers:

$$A + \mathrm{D} \xrightarrow{k_a} 2\mathrm{D}, \quad A + \mathrm{L} \xrightarrow{k_a} 2\mathrm{L},$$
$$A \underset{k_d}{\overset{k_n}{\rightleftharpoons}} \mathrm{D}, \quad A \underset{k_d}{\overset{k_n}{\rightleftharpoons}} \mathrm{L}. \tag{9}$$

Compared to Frank's model, the chiral inhibition is replaced by reversible linear decay reactions which model both recycling and nonautocatalytic production. The rate constants are denoted by k, with the subscript serving to identify the particular reaction (subscript a for autocatalysis, d for decay, and n for nonautocatalytic production). The only deterministic fixed point of this model is the racemic state [see Fig. 2(c)]. This model can be interpreted as a model for the evolution of early life where primitive chiral self-replicators can be produced randomly through nonautocatalytic processes at very low rates; the self-replication is modeled by autocatalysis while the decay reaction is a model for the death process.

It is important to note that for the nonautocatalytic reaction to occur at a very small rate compared to the decay rate, the self-replication process should be an energy-consuming reaction (as is the case in biological systems). Hence, in order to maintain an irreversible self-replication, the system has to be driven by an external source of energy. This constant inflow of energy keeps the steady state of the system far from equilibrium. The source of this driving energy is not included in our model, as is usually the case in nonequilibrium problems. For more details on the thermodynamics of this model see Sec. II D.

Section II B derives an exactly solvable stochastic differential equation for the time evolution of the chiral order parameter ω from reactions (9), which shows that in the regime where autocatalysis is the dominant reaction, the functional form of the multiplicative intrinsic noise from autocatalytic reactions stabilizes the homochiral states.

B. Master equation, Fokker-Planck equation, and Langevin equation

Chemical reactions are inherently stochastic, as they rely on the stochastic collision of molecules with sufficient energy to overcome the activation energy. The goal of this section is to derive a master equation for the rate of change of probability of the system being at a state defined by the concentration of A, D, and L molecules and a stochastic differential equation for the rate of change of the chiral order parameter ω.

Consider reactions (9) taking place in a well-mixed system of volume V with total number of molecules N. The state of the system is defined by the concentration vector $(a,d,l) \equiv (x_1,x_2,x_3) \equiv \vec{x}$ of the molecules A, D, and L, respectively. We define the transition rate $T(\vec{y}|\vec{x})$ as the probability per unit time per unit volume of the system transitioning to the state $\vec{y}$, given the initial state $\vec{x}$. From reaction (9), there are four types of transitions characterized by the four rows of the stoichiometry matrix $\mathbf{S}$:

$$\mathbf{S} = \begin{pmatrix} -1 & 1 & 0 \\ -1 & 0 & 1 \\ 1 & -1 & 0 \\ 1 & 0 & -1 \end{pmatrix}, \tag{10}$$

corresponding to the reactions that consume A, and produce D or L, respectively, and the ones that consume D or L and produce A respectively. The columns of $\mathbf{S}$ correspond to the species A, D, and L respectively, and the negative or positive signs refer to consumption or production. From the law of mass action, the transition rates corresponding to different types of transitions are given by

$$\begin{aligned} T(\vec{x} + \epsilon\vec{s}_1|\vec{x}) &= (k_n + k_a d)a, \\ T(\vec{x} + \epsilon\vec{s}_2|\vec{x}) &= (k_n + k_a l)a, \\ T(\vec{x} + \epsilon\vec{s}_3|\vec{x}) &= k_d d, \\ T(\vec{x} + \epsilon\vec{s}_4|\vec{x}) &= k_d l, \end{aligned} \tag{11}$$

where the vector $\vec{s}_i$ (with $i = 1,\ldots,4$) is the ith row of the stoichiometry matrix $\mathbf{S}$, $\epsilon = 1/V$ is one over the volume V of the system, $\epsilon\vec{s}_i$ are the changes in the concentration vector $\vec{x}$ due to a reaction of type i.

Now, the rate of change of the probability of the system being at a state $\vec{x}$ at time t, $P(\vec{x},t)$, is given by

$$\frac{\partial P(\vec{x},t)}{\partial t} = V \sum_{\vec{y}} [T(\vec{x}|\vec{y})P(\vec{y},t) - T(\vec{y}|\vec{x})P(\vec{x},t)]. \tag{12}$$

Equation (12) is called the master equation [42], and it describes the time evolution of probability of the system at a state defined by discrete concentration values. The master equation is the most accurate description of the individual level model and can be simulated exactly using the Gillespie algorithm [43]. In the master equation for reaction (9), most of the transition rates are zero, except the allowed transitions specified by Eq. (11). Substituting the allowed transitions from Eq. (11) in Eq. (12), we obtain

$$\begin{aligned} \frac{\partial P(\vec{x},t)}{\partial t} = V \sum_{i=1}^{4} &[T(\vec{x}|\vec{x} - \epsilon\vec{s}_i)P(\vec{x} - \epsilon\vec{s}_i,t) \\ &- T(\vec{x} + \epsilon\vec{s}_i|\vec{x})P(\vec{x},t)]. \end{aligned} \tag{13}$$

The next step is to take the continuous limit of Eq. (12) when the total number of molecules $N \gg 1$, to derive a partial differential equation for the time evolution of the probability density of finding the system in a state defined by continuous concentration variables. This equation in known as the *Fokker-Planck equation.* We begin by defining the functions F_i as

$$F_i(\vec{x},t) = T(\vec{x}|\vec{x} + \epsilon\vec{s}_i)P(\vec{x},t), \tag{14}$$

so that the master equation can be written as

$$\frac{\partial P(\vec{x},t)}{\partial t} = \sum_{i=1}^{4} \frac{F_i(\vec{x} - \epsilon\vec{s}_i,t) - F_i(\vec{x},t)}{\epsilon}. \tag{15}$$

The right-hand side of the master equation can be expanded in ϵ:

$$\frac{\partial P(\vec{x},t)}{\partial t} = -\sum_{i,j} S_{i,j}\frac{\partial F_i}{\partial x_j} + \frac{\epsilon}{2}\sum_{i,j,k} S_{i,j}S_{i,k}\frac{\partial^2 F_i}{\partial x_j \partial x_k} - \frac{\epsilon}{6}\sum_{i,j,k,l} S_{i,j}S_{i,k}S_{i,l}\frac{\partial^3 F_i}{\partial x_j \partial x_k \partial x_l} + \cdots . \quad (16)$$

If $P(\vec{x},t)$ is analytic in ϵ, before truncation, Eq. (16) is exact and does not require ϵ to be small. For $N \gg 1$, by the central limit theorem, the fluctuations are Gaussian, and therefore, the probability density function $P(\vec{x},t)$ has to obey a second order Fokker-Planck equation. At this limit, even if ϵ is not small, we can truncate the series to second order, and after evaluating the corresponding partial derivatives, we obtain the following Fokker-Planck equation for the time evolution of $P(\vec{x},t)$:

$$\frac{\partial P}{\partial t} \approx -\sum_{j=1}^{3}\frac{\partial (H_j P)}{\partial x_j} + \frac{1}{2}\sum_{j,k=1}^{3}\frac{\partial^2 (B_{jk}P)}{\partial x_j \partial x_k}, \quad (17)$$

where the drift vector $\vec{H}$ with component H_j is given by

$$\vec{H} = \sum_i T(\vec{x}+\epsilon\vec{s}_i|\vec{x})\vec{s}_i = \begin{pmatrix} k_d(d+l) - a(2k_n + k_a(d+l)) \\ -k_d d + a(k_n + k_a d) \\ -k_d l + a(k_n + k_a l) \end{pmatrix}. \quad (18)$$

The symmetric diffusion matrix $\mathbf{B}$ is given by

$$\mathbf{B} = \epsilon\sum_i T(\vec{x}+\epsilon\vec{s}_i|\vec{x})\vec{s}_i \otimes \vec{s}_i = \epsilon\begin{pmatrix} k_d(d+l)+a(2k_n+k_a(d+l)) & -k_d d - a(k_n+k_a d) & -k_d l - a(k_n + k_a l) \\ -k_d d - a(k_n + k_a d) & k_d d + a(k_n + k_a d) & 0 \\ -k_d l - a(k_n + k_a l) & 0 & k_d l + a(k_n + k_a l) \end{pmatrix}, \quad (19)$$

where the symbol $\otimes$ indicates the Kronecker product.

Equation (17) describes the time evolution of the probability density of the concentration vector $\vec{x}$ in the continuous model, and all further approximations and simplifications can be done directly on this equation. However, it is more insightful to keep track of the stochastic dynamics of the concentration variables. The following is the set of stochastic differential equations (defined in the Itō sense; see Ref. [37]) corresponding to a probability density function obeying Eq. (17):

$$\frac{d\vec{x}}{dt} = \vec{H}(\vec{x}) + \vec{\xi}(t), \quad (20)$$

where ξ_i, the components of $\vec{\xi}(t)$, are zero mean Gaussian noise functions with correlation

$$\langle \xi_i(t)\xi_j(t')\rangle = B_{i,j}\delta(t-t'). \quad (21)$$

To rewrite Eq. (20) in terms of uncorrelated Gaussian noise functions, we seek to decompose the matrix $\mathbf{B}$ to $\mathbf{B} = \mathbf{G}\mathbf{G}^{\mathsf{T}}$. This decomposition is not unique and multiple choices for $\mathbf{G}$ exist [44]. It is easy to check that the following 3×2 matrix satisfies the decomposition:

$$\mathbf{G} = \sqrt{\epsilon}\begin{pmatrix} \sqrt{a(k_a d + k_n) + k_d d} & \sqrt{a(k_a l + k_n) + k_d l} \\ -\sqrt{a(k_a d + k_n) + k_d d} & 0 \\ 0 & -\sqrt{a(k_a l + k_n) + k_d l} \end{pmatrix}. \quad (22)$$

For more details on how such decompositions are found, see Appendix A. Now, for a two-dimensional zero mean Gaussian white noise $\vec{\eta}(t)$ with correlation

$$\langle \eta_j(t)\eta_k(t')\rangle = \delta_{j,k}\delta(t-t'), \quad (23)$$

the correlated noise $\vec{\xi}(t)$ can be rewritten as $\vec{\xi}(t) = \mathbf{G}\vec{\eta}(t)$ (see Appendix A). Now, Eq. (20) can be written in terms of $\vec{\eta}$ as

$$\frac{d\vec{x}}{dt} = \vec{H}(\vec{x}) + \mathbf{G}(\vec{x})\vec{\eta}(t). \quad (24)$$

Note that since the Fokker-Planck equation (17) only depends on $\mathbf{B}$ and not the particular choice of its decomposition $\mathbf{G}$, the probability density function of $\vec{x}$ and its time evolution do not depend on $\mathbf{G}$ either [44].

To obtain a stochastic differential equation for the time evolution of the chirality order parameter ω, we perform the following change of variables in Eq. (24):

$$\begin{pmatrix} a \\ d \\ l \end{pmatrix} \to \begin{pmatrix} n \\ r \\ \omega \end{pmatrix} = \begin{pmatrix} a+d+l \\ d+l \\ (d-l)/(d+l) \end{pmatrix}. \quad (25)$$

Using Itō's lemma [37] we can obtain an equation for the time evolution of the new state vector $\vec{y} = (n,r,\omega)$.

In general, it is not easy to solve for the joint probability density of coupled stochastic differential equations (SDE), but for a single variable first order SDE the steady state distribution is always exactly solvable. Therefore, we seek to reduce the number of degrees of freedom in the problem using the following two facts:

(1) The reaction scheme reaction (9) conserves the total number of molecules, meaning that the total concentration $n = a + d + l$ is constant.

(2) Simulations show that the concentration $r = d + l$ settles to a Gaussian distribution around its fixed point value r^*, allowing us to substitute $r(t) \to r^*$. Therefore, the dynamics at long time occurs only in the chiral order parameter ω.

In the new variables, we find that $\dot{n} = 0$, and, by taking the positive solution of $\dot{r} = 0$, that is

$$r^* = \frac{\sqrt{(k_a n - k_d - 2k_n)^2 + 8k_a k_n n} + k_a n - k_d - 2k_n}{2k_a}, \quad (26)$$

we substitute $r \to r^*$ in the equation for ω, and use the rule for summing Gaussian variables (i.e., $a\eta_1 + b\eta_2 = \sqrt{a^2+b^2}\eta$; where a and b are generic functions [37]) to express the stochastic part of the equation using a single noise variable.

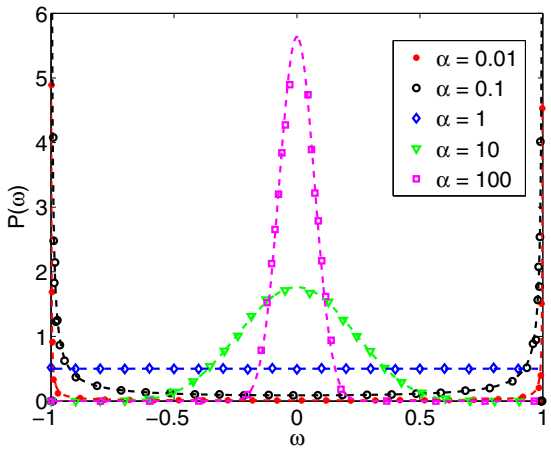

FIG. 3. Comparison between the stationary distribution, Eq. (29), (dashed lines) and Gillespie simulations of reactions reaction (9) (markers), for different values of α. Simulation parameters: $N = 10^3$, $k_a = k_n = k_d = 1$.

Expressing the result in terms of the total number of molecules $N = Vn$, for $N \gg 1$, we arrive at the following stochastic differential equation for the chiral order parameter ω:

$$\frac{d\omega}{dt} = -\frac{2k_n k_d V}{N k_a}\omega + \sqrt{\frac{2k_d}{N}(1-\omega^2)}\eta(t), \qquad (27)$$

where $\eta(t)$ is Gaussian white noise with zero mean and unit variance. The time evolution of the probability density function of ω is described by the corresponding Fokker-Planck equation of Eq. (27) given by

$$\frac{\partial P(\omega,t)}{\partial t} = \frac{\partial}{\partial \omega}\left[\frac{2k_n k_d V}{N k_a}\omega P(\omega,t)\right] + \frac{1}{2}\frac{\partial^2}{\partial \omega^2}\left[\frac{2k_d}{N}(1-\omega^2)P(\omega,t)\right]. \qquad (28)$$

This is an exactly solvable partial differential equation with time-dependent solution given in [45]. The steady state solution of Eq. (28) is given by

$$P_s(\omega) = \mathcal{N}(1-\omega^2)^{\alpha-1}, \quad \text{with} \quad \alpha = \frac{k_n V}{k_a}, \qquad (29)$$

with the normalization constant

$$\mathcal{N} = \left[\int_{-1}^{+1}(1-\omega^2)^{\alpha-1}d\omega\right]^{-1} = \frac{\Gamma\left(\alpha+\frac{1}{2}\right)}{\sqrt{\pi}\,\Gamma(\alpha)}. \qquad (30)$$

Equation (29) is compared in Fig. 3 against exact Gillespie simulations [43] of reactions (9). For $\alpha = \alpha_c = 1$, ω is uniformly distributed. For $\alpha \gg \alpha_c$, where the nonautocatalytic production is the dominant production reaction, $P_s(\omega)$ is peaked around the racemic state, $\omega = 0$. For $\alpha \ll \alpha_c$, where autocatalysis is dominant, $P_s(\omega)$ is sharply peaked around the homochiral states, $\omega = \pm 1$. The simulations were performed for $N = 1000$, where the analytic theory is expected to be accurate; for much smaller values of N, the theory is qualitatively correct, but very small quantitative deviations are observable compared to the simulations.

For finite N and nonzero α smaller than one, the system can switch from one homochiral state to the other over long time. The expected value of this switching time approaches infinity for large N and small α. See Appendix B for the calculation of the mean switching time and analytical expressions.

The importance of this treatment is not only in the analytical results for the probability density function of ω, but also the intuitive picture that Eq. (27) provides to understand the mechanism through which autocatalysis leads to homochirality. We will discuss an intuitive interpretation of Eq. (27) and the behavior of its solution Eq. (29) in Sec. II C along with the relationship of this model with the origin of life.

C. Transition to homochirality and origin of life

In Sec. II B we saw that for the reactions (9), in a well-mixed system of volume V and total number of molecules N, the time evolution of the chiral order parameter ω obeys the stochastic differential equation

$$\frac{d\omega}{dt} = -\frac{2k_n k_d V}{N k_a}\omega + \sqrt{\frac{2k_d}{N}(1-\omega^2)}\eta(t), \qquad \text{(27 revisited)}$$

where $\eta(t)$ is a normalized Gaussian white noise with zero mean defined in the Itō sense [37]. The deterministic part of Eq. (27)

$$\frac{d\omega}{dt} = -\frac{2k_n k_d V}{N k_a}\omega, \qquad (31)$$

which could alternatively be derived by reaction kinetic analysis (see Sec. I C), has one stable fixed point at the racemic state, consistent with the phase portrait in Fig. 2(c). The multiplicative noise in Eq. (27) vanishes at homochiral states and admits its maximum at the racemic state. In order to determine which one of the two terms is dominant, one can define the dimensionless parameter α as the ratio of the two constants $2k_n k_d V/Nk_a$ and $2k_d/N$, that is,

$$\alpha = \frac{k_n V}{k_a}. \qquad (32)$$

It can also be seen in Eq. (28) that α is the ratio that determines which term is dominant. Note that the steady state solution of Eq. (27), given in Eq. (29), depends only on α. When $\alpha \gg 1$, the deterministic part of the Eq. (27) is dominant, and therefore, we expect a racemic solution. That is indeed the case, and the steady state probability density of ω is peaked around zero for large α (see Fig. 3). However, for $\alpha \ll 1$, where autocatalysis is the dominant production mechanism, the amplitude of the noise term in Eq. (27) is much larger than the amplitude of the corresponding deterministic term. Since the noise is maximum at the racemic state, the variable ω stochastically walks away from the racemic state over time and ends up at homochiral states where the noise term vanishes.

To understand this result physically, note that the source of the multiplicative noise is the intrinsic stochasticity of the autocatalytic reactions. While, on average, the two autocatalytic reactions do not change the variable ω [see Fig. 2(b)], each time one of the reactions takes place, the value of ω changes by a very small discrete amount. As a result, over time the value of ω drifts away from its initial value. Since the amplitude of the noise term is maximum at racemic state and zero at homochiral states, this drift stops at one of the homochiral states.

The absence of the noise from autocatalysis at homochiral states can be understood by recognizing that at homochiral states, the molecules with only one of two chiral states D and L are present, hence only the autocatalytic reaction associated with that chiral state has a nonzero rate. This reaction produces molecules of the same chirality, keeping the system at the same homochiral state without affecting the value of ω, and therefore, the variable ω does not experience a drift away from the homochiral states due the autocatalytic reactions.

Note that the stationary distribution of ω in Eq. (29) is dependent only on α and is independent of the decay reaction rate, k_d. The only role of this reaction is to prevent the A molecules from being completely consumed, thus providing a well-defined nonequilibrium steady state independent of the initial conditions.

The parameter α is proportional to the ratio of the nonautocatalytic production rate, k_n, to the self-replication rate, k_a. In the evolution of early life, when self-replication was a primitive function, k_a would be small and the value of α would therefore be large. As life evolved, the self-replicators would evolve to become more efficient at self-replication and would be less likely to be produced spontaneously through non-self-replicating mechanisms. As a result the value of k_a would increase, while k_n decrease, and α would become very small. Therefore, in our model, we expect that life started in a racemic state, and it transitioned to homochirality after self-replication became efficient (i.e., when $\alpha \ll 1$). It is a necessary weakness of the present state of understanding that we do not have a dynamical description of $\alpha(t)$, so in this sense, our theory is incomplete.

It is important to note that all of the previous mechanisms suggested for homochirality rely on assumptions that cannot be easily confirmed to hold during the emergence of life. However, even if all of such mechanisms fail during the origin of life, our mechanism guarantees the emergence of homochirality, since it only relies on self-replication and death, two processes that are inseparable from any living system.

D. Pigs *can* fly (with jetpacks): Violation of detailed balance is a necessary condition for homochirality

By construction, our model violates the principle of microscopic reversibility, and in this section, we wish to comment on this fact and explore its physical origin. The violation of microscopic reversibility follows because our model explicitly violates the principle of detailed balance, as is required for an externally driven system far from equilibrium. Here we review some thermodynamical aspects of our model, which we believe have important implications for understanding the origin of life. Before starting to analyze the model, we would like to review the history of criticisms to minimal models for homochirality that violate microscopic reversibility.

In 2009, Blackmond published an essay titled *"If pigs could fly" chemistry: A tutorial on the principle of microscopic reversibility* [46]. The essay criticizes several kinetic models of homochirality similar to Frank's model, with the type of recycling that exists in our model. Blackmond argues that these kinetic models are written with arbitrary reactions constants without a regard for whether reactions with these constants are thermodynamically feasible or not. The crux of the argument boils down to the following: *the principle of microscopic reversibility* states that at equilibrium, the rate of the forward reaction and the reverse reaction are equal for all reactions. For systems involving recycling, or more generally cyclic reactions, this principle puts a constraint on the relationship of the rate constants of the set of reactions that share their pool of reactants and products. For example, consider the cyclic reaction set

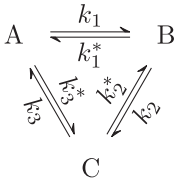

(33)

At equilibrium, the rate of forward and backward reactions are the same for each reaction, giving rise to the following relationships:

$$k_1[A] = k_1^*[B], \quad k_2[B] = k_2^*[C], \quad k_3[C] = k_3^*[A]. \tag{34}$$

Eliminating the concentrations $[A]$, $[B]$, and $[C]$, we have

$$\frac{k_1}{k_1^*}\frac{k_2}{k_2^*}\frac{k_3}{k_3^*} = 1. \tag{35}$$

This relationship was discovered by Wegscheider in 1901 [47]. It implies that, at equilibrium, the six reaction rates cannot be chosen independently. In particular, one cannot have a set of cyclic irreversible reactions, that is, for nonzero k_1, k_2, and k_3, we cannot set k_1^*, k_2^*, and k_3^* simultaneously to zero, at equilibrium. Of course, once a static equilibrium solution exists, these constants should obey Wegscheider's conditions, even away from the steady state, such as during the approach to equilibrium. This is because reaction constants are constants, i.e., independent of the extent of reactions. In other words, Wegscheider's condition is the condition for the existence of a static equilibrium solution. The principle of microscopic reversibility entails that the steady state solution satisfies detailed balance, i.e., it is an equilibrium state. If a model has an equilibrium solution, one can derive the rate constants from the free energy differences. However, in a cyclic reaction set, not all the free energy differences are independent. As a result, for a model to have an equilibrium solution, its rate constants have to obey a constraint, and that is Wegscheider's condition.

What does it all have to do with homochirality? There is a similar situation in the model defined by reactions (9) because of the recycling and irreversibility of the autocatalytic reactions. Note that the linear and the autocatalytic reactions have the same reactants and products, therefore, doing the same analysis on reactions

$$A + \mathrm{D} \underset{k_a^*}{\overset{k_a}{\rightleftharpoons}} 2\mathrm{D}, \quad A \underset{k_d}{\overset{k_n}{\rightleftharpoons}} \mathrm{D}, \tag{36}$$

results in the following condition at equilibrium:

$$k_a[A][\mathrm{D}] = k_a^*[\mathrm{D}]^2, \quad k_n[A] = k_d[\mathrm{D}], \tag{37}$$

which implies

$$\frac{k_a}{k_a^*} = \frac{k_n}{k_d}. \tag{38}$$

This suggests that for this model to have an equilibrium solution, it cannot have an irreversible autocatalysis and recycling simultaneously (i.e., k_a^* cannot be zero for a nonzero k_d).

Is this a potential source of criticism against our model? After all, it might seem that every set of chemical reactions should have a static equilibrium. In fact this is not the case: every *closed* set of chemical reactions should have a static equilibrium. We have made it clear that the stationary solution of our model is a nonequilibrium steady state, and therefore, it has to be a driven system with an external source of energy or disequilibrium. In fact, as we will show in this section, any system modeling prebiotic chemistry, and more importantly any model attempting to achieve complete homochirality has to be a driven model. Like Frank and most other workers in this field, we chose not to include the external source of energy in our model for several reasons: (1) it is unnecessary and not the main point of the exercise; (2) it forces us to make specific and detailed choices about chemical processes that have no experimental support in an early life context; and (3) it obscures the basic mechanisms leading to homochirality.

Before we show why it is necessary for there to be an external source of energy, in order to give rise to a homochiral steady state, let us mention a couple of different ways one can implement such energy sources, keeping the autocatalysis irreversible.

The reaction set (9) was set up with the idea in mind that self-replication (modeled by the autocatalytic reactions) has exclusive access to an external source of energy, as is the case in all biological systems, and therefore the effective "reaction constants" (which are dependent on the amount of energy to which the replicator has access) can be tuned independently of the other nonautocatalytic reactions. This can be shown by adding extra molecular species representing the source of energy.[5] For example, modern organisms couple the hydrolysis reaction of adenosine triphosphate (ATP) that produces adenosine diphosphate (ADP) and a phosphate (P) to their autocatalytic cycles in their cells, using the free energy difference to drive the cycles [48]. Consider the following set of reactions:

$$\begin{aligned} &A + \mathrm{D} + ATP \xrightarrow{k_s} 2\mathrm{D} + ADP + P, \\ &A + \mathrm{L} + ATP \xrightarrow{k_s} 2\mathrm{L} + ADP + P, \\ &A \underset{k_d}{\overset{k_n}{\rightleftharpoons}} \mathrm{D}, \quad A \underset{k_d}{\overset{k_n}{\rightleftharpoons}} \mathrm{L}. \end{aligned} \tag{39}$$

These reaction rates are independent of each other. Now, keeping the concentration of ATP constant (by providing a constant supply of ATP), the self-replication reactions can be written in the compact form

$$A + \mathrm{D} \xrightarrow{k_s[ATP]} 2\mathrm{D}, \quad A + \mathrm{L} \xrightarrow{k_s[ATP]} 2\mathrm{L}, \tag{40}$$

ignoring the inactive compounds, ADP and P. Now we can simply define an *effective* reaction rate $k_a = k_s[ATP]$, recovering reactions (9). This reaction rate, as promised, is tunable independently of the other reaction constants; it depends on the availability of the energy source.

Another potential solution to this problem is to change the set of proposed reactions to

$$\begin{aligned} &A + \mathrm{D} \xrightarrow{k_a} 2\mathrm{D}, \quad \mathrm{D} \underset{k_n}{\overset{k_d}{\rightleftharpoons}} B, \\ &A + \mathrm{L} \xrightarrow{k_a} 2\mathrm{L}, \quad \mathrm{L} \underset{k_n}{\overset{k_d}{\rightleftharpoons}} B. \end{aligned} \tag{41}$$

In this model, D and L enantiomers are autocatalytically produced from a less stable achiral molecule A and decay to a more stable achiral molecule B. Now, all we need to do to drive the reactions to a nonequilibrium steady state is to provide a constant supply of A and continuously remove B from the system. The free energy difference between A and B will provide the driving force. Of course, this solution only moves the nonequilibrium driving from the original reactions to the precise mechanism that supplies A and removes B from the system. Unlike the previous solution, this is a different model with slightly different kinetics. However, it does result in a homochiral steady state through the same exact noise-induced mechanism described in this section. That attests to the fact that our mechanism only depends on self-replication and decay, and the details of the chemical reactions implementing these processes are irrelevant. There are other ways to model the source of driving energy in the system; see, for example, Ref. [49] for a resolution of a similar problem in another model of homochirality.

A steady process of self-replication requires a constant supply of energy, and therefore, an open system. This is true of all biological systems today, and so has to have been true during the emergence of life. In general the source of energy for self-replication could be a constant supply of high free energy molecules, steady flow of photons from sunlight, voltage difference across an alkaline hydrothermal vent in the bottom of the ocean, or any perhaps unknown kind of interesting chemistry that led to the emergence of life. These cases may all look like "exceptional cases" compared to typical test tube experiments done in the laboratory, but it would be hard to imagine a scenario for the origin of life that does not involve an external driving force.

The fact that biological systems are driven is not the only reasoning behind open driven models for homochirality. In fact there are thermodynamical constraints on the type of model that could lead to complete homochirality. Perhaps the most straightforward argument for open driven models of homochirality with recycling is the following: it is a well-known fact that amino acids spontaneously racemize over the time scale of years to millennia depending on temperature and pH [3,50,51]. Note that this is a very short time scale compared to geological time scales associated with the origin of life. Any mechanism for homochirality that does not continuously recycle the product will end up with a racemic equilibrium mixture of amino acids. Of course a continuous recycling and production through a separate mechanism requires a steady

[5]The presence of additional molecules species is not strictly necessary, as the source of energy could be nonmolecular in nature. Photoactive chemical reactions are examples of energy-driven systems, whose energy source is not molecular.

supply of external driving force leading to a nonequilibrium steady state.

This argument goes deeper than amino acids: there is no closed dilute[6] system with a completely homochiral equilibrium. Suppose that the equilibrium state of a system is homochiral for at least one type of the chiral molecules in the system. Let us make a replica of the system and replace half of those chiral molecules with their mirror images. This transformation does not change the internal energy, U, of the system, since both of the chiral molecules have the same internal energy. It does not change the pressure or the volume of the system either, since all the physical properties of the two chiral molecules are identical by symmetry. However, the entropy of the racemic replica is larger than that of the homochiral system. Therefore, the Gibbs free energy, $G = U + pV - TS$, of the racemic mixture is lower than that of homochiral mixture, and the homochiral solution cannot be the equilibrium solution of the system; over long time, such homochiral solution will racemize. Only a continuously driven mechanism can keep such system in a homochiral state over long time, and that state will be a nonequilibrium steady state.

III. NOISE-INDUCED HOMOCHIRALITY IN SPATIALLY EXTENDED SYSTEMS

Let us suppose for the moment that life started through autocatalytic reactions in alkaline hydrothermal vents in the bottom of the ocean [52] (this is just an example, and what follows does not depend on the details of the origin of life scenario). Now, whatever symmetry-breaking mechanism we propose for the origin of homochirality in this prebiotic world should be robust in the following sense: First, consider two nearby hydrothermal vents. In the absence of diffusion, over time, each one becomes homochiral through some symmetry-breaking mechanism. This homochirality should be robust with respect to the perturbation caused by, e.g., molecules of opposite chirality diffusing from the other vent. Second, over time the particular choice of homochirality should be synchronized over all of the sources of production of these chiral molecules.

In this section, we will show that the noise-induced homochirality mechanism suggested in Sec. II is robust with respect to these two criteria. In Sec. III A we define the spatial extension of our model as a set of well-mixed reaction patches diffusively coupled to their neighbors. The Fokker-Planck equation for two diffusively coupled patches is derived in Sec. III B, followed by a perturbation theory analysis in Sec. III C, showing the first robustness criterion for our model holds when autocatalysis is the dominant production mechanism. In Sec. III D we study the one-dimensional spatial extension of the model in the continuum limit, where we see that the correlation length for the chiral order parameter diverges as the nonautocatalytic reaction rates approaches zero. Moreover, we show simulation results for a one-dimensional system of diffusively coupled patches at pure autocatalytic limit, where the patches synchronize their final homochiral state. This indicates that the pure autocatalytic limit of our model is robust with respect to the second robustness criterion.

A. Description of the spatially extended model

Consider the following spatial extension [53] of the model described in Sec. II: let reactions (9) take place in a set of M well-mixed patches of volume V, while molecules can diffuse between neighboring patches with diffusion rate δ. The set of neighbors of each patch i, $i = 1, \ldots, M$, is denoted by $\langle i \rangle$ (e.g., for a linear chain, $\langle i \rangle = \{i-1, i+1\}$) and molecules of species A, D, and L in patch i by A_i, D_i, and L_i respectively. In summary, the following set of reactions defines the spatial model:

$$
\begin{aligned}
&A_i \underset{k_d}{\overset{k_n}{\rightleftharpoons}} \mathrm{D}_i, \quad A_i \underset{k_d}{\overset{k_n}{\rightleftharpoons}} \mathrm{L}_i, \quad i = 1, \ldots, M,\\
&A_i + \mathrm{D}_i \xrightarrow{k_a} 2\mathrm{D}_i, \quad A_i + \mathrm{L}_i \xrightarrow{k_a} 2\mathrm{L}_i,\\
&\mathrm{D}_i \overset{\delta}{\rightleftharpoons} \mathrm{D}_j, \quad \mathrm{L}_i \overset{\delta}{\rightleftharpoons} \mathrm{L}_j, \quad j \in \langle i \rangle.
\end{aligned} \tag{42}
$$

A similar analytical treatment to that of Sec. II B results in the following set of coupled stochastic differential equations for the time evolution of the chiral order parameter ω_i, of each patch i (we will see a step by step derivation of the special case $M = 2$ in Sec. III B):

$$
\begin{aligned}
\frac{d\omega_i}{dt} = &-\frac{2k_n k_d V}{N k_a}\omega_i + \delta \sum_{j\in\langle i\rangle}(\omega_j - \omega_i)\\
&+ \sqrt{\frac{2k_d}{N}\left(1-\omega_i^2\right)}\eta_i(t) + \sqrt{\frac{\delta}{N}}\xi_i(\vec{\omega},t),
\end{aligned} \tag{43}
$$

where now N represents the average number of molecules per patch, η_i are independent normalized Gaussian white noises, ξ_i are zero mean Gaussian noise with correlation

$$
\begin{aligned}
\langle \xi_i(t)\xi_j(t')\rangle = \Bigg[&2\sum_{k\in\langle i\rangle}(1-\omega_i\omega_k)\delta_{i,j}\\
&+ \left(\omega_i^2 + \omega_j^2 - 2\right)\chi_{\langle i\rangle}(j)\Bigg]\delta(t-t'),
\end{aligned} \tag{44}
$$

and $\chi_{\langle i\rangle}(j)$ is equal to one if $j \in \langle i\rangle$ and zero otherwise.

B. Two-patch model: Fokker-Planck equation

Let us analyze the homochirality in each patch of the spatial extension of our model described by reactions (42) with $M = 2$. We can follow the procedure explained in Sec. II B to obtain a Fokker-Planck equation for the time evolution of

[6]The diluteness assumption is implicit in many of these types of arguments. For example the idea that one can deduce the rate constant from the free energy difference to use in the law of mass action depends on the assumption that there is a free energy per molecule independent of the concentrations of other molecules (otherwise, this rate constant will not be constant and will depend on the extends of all reactions in the system. The Wegscheider condition does not hold in such case, even when there exist a well-defined equilibrium). This assumption is valid only when we ignore the interactions in the system, which can be done for dilute systems. The argument of this paragraph without the diluteness condition will completely fail, for example, in homochiral crystals that can be stable as a closed systems.

the probability density of the system being at a state with concentrations a_1, d_1, l_1, a_2, d_2, and l_2. Again we can reduce the number of variables using the following facts: (1) the total concentration $n_t = n_1 + n_2 = a_1 + d_1 + l_1 + a_2 + d_2 + l_2$ is conserved; and (2) simulation shows that in long time, the variables $r_1 = d_1 + l_1$, $r_2 = d_2 + l_2$, and $\Delta = n_1 - n_2$ settle to Gaussian distributions around their fixed point values $r_1 = r_2 = r^*$ and $\Delta = 0$. We make the following change of variables:

$$\begin{pmatrix} a_1 \\ d_1 \\ l_1 \\ a_2 \\ d_2 \\ l_2 \end{pmatrix} \to \begin{pmatrix} n_t \\ \Delta \\ r_1 \\ r_2 \\ \omega_1 \\ \omega_2 \end{pmatrix} = \begin{pmatrix} a_1 + d_1 + l_1 + a_2 + d_2 + l_2 \\ a_1 + d_1 + l_1 - a_2 - d_2 - l_2 \\ d_1 + l_1 \\ d_2 + l_2 \\ (d_1 - l_1)/(d_1 + l_1) \\ (d_2 - l_2)/(d_2 + l_2) \end{pmatrix} \tag{45}$$

using Itō's formula. Now the dynamics occurs only in $\vec{\omega} = (\omega_1, \omega_2)$. For large average number of molecules per patch $N \gg 1$, the resulting Fokker-Planck equation for the time evolution of the joint probability density function of ω_1 and ω_2, $Q(\vec{\omega}, t)$, reads

$$\frac{\partial Q}{\partial t} = -\sum_{i=1}^{2} \frac{\partial((\mathbf{L}\vec{\omega})_i Q)}{\partial \omega_i} + \frac{1}{2} \sum_{i,j=1}^{2} \frac{\partial^2 (U_{ij} Q)}{\partial \omega_i \partial \omega_j}. \tag{46}$$

Note that the above sums are now over the patches, and not over species as in Eq. (17). The Jacobian matrix $\mathbf{L}$ is given by

$$\mathbf{L} = -\frac{2k_d k_n V}{N k_a} \begin{pmatrix} 1 & 0 \\ 0 & 1 \end{pmatrix} + \delta \begin{pmatrix} -1 & 1 \\ 1 & -1 \end{pmatrix}, \tag{47}$$

and the diffusion matrix $\mathbf{U}$ by

$$\mathbf{U} = \frac{2k_d}{N} \begin{pmatrix} 1 - \omega_1^2 & 0 \\ 0 & 1 - \omega_2^2 \end{pmatrix} + \frac{\delta}{N} \begin{pmatrix} 2(1 - \omega_1\omega_2) & \omega_1^2 + \omega_2^2 - 2 \\ \omega_1^2 + \omega_2^2 - 2 & 2(1 - \omega_1\omega_2). \end{pmatrix}. \tag{48}$$

This Fokker-Planck equation describes the time evolution of the probability density of stochastic variables obeying the spacial case, $M = 2$, of Eq. (43).

C. Two-patch model: Homochirality

Does a system described by reactions (9) stay homochiral when diffusively coupled to similar systems? To answer this question, we need to analyze the homochirality in each patch of the spatial extension of our model described by reactions (42) with $M = 2$. In Sec. III B, we showed that the joint probability density of chiral order parameters of two diffusively coupled patches obeys Eq. (46). The probability density function of the chiral order parameter of a single patch, $Q_s(\omega)$ is defined by

$$Q_s(\omega) = \int_{-1}^{+1} Q_s(\omega, \omega_2)\, d\omega_2 = \int_{-1}^{+1} Q_s(\omega_1, \omega)\, d\omega_1, \tag{49}$$

where $Q_s(\omega_1, \omega_2)$ is the stationary solution of Eq. (46). We first analyze the condition for each patch reaching homochirality using perturbation theory, in the case of slow diffusion. For $\delta \sim k_d/N$ or smaller, we can treat the diffusion deterministically by ignoring the last term in Eq. (48). To solve for $Q_s(\omega)$, we begin by rewriting Eq. (46) as a continuity equation,

$$\partial_t Q + \nabla \cdot \vec{J} = 0, \tag{50}$$

which defines the probability current $\vec{J}$ as [37]

$$\vec{J} = \mathbf{L}\vec{\omega}\, Q - \tfrac{1}{2} \nabla \cdot (\mathbf{U} Q). \tag{51}$$

By the conservation of probability, at steady state, the total probability flux $\vec{J}_s$ through each vertical section of ω_1-ω_2 plane must be zero:

$$\begin{aligned} \int_{-1}^{+1} J_{s,1} d\omega_2 &= \int_{-1}^{+1} \left[(\mathbf{L}\vec{\omega})_1 Q_s - \frac{1}{2} \partial_{\omega_1} (U_{11} Q_s) \right] d\omega_2 \\ &= Q_s(\omega_1)\omega_1 \left[\frac{2k_d}{N}(1 - \alpha) - \delta \right] \\ &\quad - \frac{k_d}{N}(1 - \omega_1^2) \frac{dQ_s}{d\omega_1} \\ &\quad + \delta \int_{-1}^{+1} \omega_2 Q_s(\omega_1, \omega_2)\, d\omega_2 = 0. \end{aligned} \tag{52}$$

The last integral can be evaluated using Bayes's theorem

$$\begin{aligned} \delta \int_{-1}^{+1} \omega_2 Q_s(\omega_1, \omega_2) d\omega_2 &= \delta \int_{-1}^{+1} \omega_2 Q_s(\omega_2|\omega_1) Q_s(\omega_1)\, d\omega_2 \\ &= \delta\ Q_s(\omega_1) \langle \omega_2 \rangle_{\omega_1} = O(\delta^2), \end{aligned} \tag{53}$$

which is of order δ^2 for small δ, since, $\langle \omega_2 \rangle_{\omega_1}$ (the expected value of ω_2 given ω_1) vanishes at zero δ, and therefore, is of order δ for small δ. In this regime, Eq. (52) provides us with a differential equation for $Q_s(\omega)$ with the solution

$$Q_s(\omega) = \mathcal{Z}(1 - \omega^2)^{\alpha + \frac{\delta N}{2k_d} - 1}, \tag{54}$$

where the normalization constant $\mathcal{Z}$ is given by

$$\mathcal{Z} = \frac{\Gamma\left(\alpha + \frac{\delta N}{2k_d} + \frac{1}{2}\right)}{\sqrt{\pi}\ \Gamma\left(\alpha + \frac{\delta N}{2k_d}\right)}. \tag{55}$$

This result shows that the critical α below which the distribution of chirality in each patch becomes bimodal, up to the first order correction in δ, is given by

$$\alpha_c \approx 1 - \delta \frac{N}{2k_d}, \quad \text{for } \delta \approx 0. \tag{56}$$

We can now turn to the case of high diffusion. Recall that the patches are defined as the maximum volume around a point in space in which the system can be considered well mixed. This can be interpreted as the maximum volume in which diffusion dominates over the other terms acting on the variable of interest (in this case ω). From Eq. (43), this condition is fulfilled for $\delta \sim 2k_d\alpha/N$. In the vicinity of the transition α is of order unity, therefore the condition becomes $\delta \sim k_d/N$. For $\delta \gg k_d/N$, the whole system can be considered well mixed and has the critical value of α, $\alpha_c^{\text{system}} = 1$, from the well-mixed results (see Sec. II B). Note that α scales with the volume, and the volume of the whole system is two times the volume of each patch, i.e., $2V$. This indicates that in a single patch

$$\alpha_c \approx \tfrac{1}{2}, \quad \text{for } \delta \gg 0. \tag{57}$$

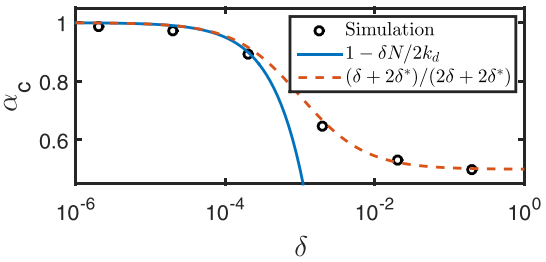

FIG. 4. Parameter α_c^{patch} in the two-patch system as a function of the diffusion rate δ. Gillespie simulations (markers) are compared against Eq. (56) (solid blue line) and Eq. (58) (dashed red line). Simulation parameters as in Fig. 3.

Now we can interpolate between these extreme limits, asymptotic to $1/2$ for large δ and to Eq. (56) for small δ:

$$\alpha_c = \frac{\delta + 2\delta^*}{2\delta + 2\delta^*}, \qquad \delta^* = \frac{k_d}{N}. \tag{58}$$

Figure 4 shows agreement between α_c measured from Gillespie simulations of the two-patch system and Eq. (58). At the parameter regime below the α_c curve in Fig. 4, individual patches are homochiral. Also, we find that the correlation between the homochiral states of the two patches increases with diffusion rate δ, and they become completely correlated when $\delta \sim k_d/N$ or more. In this regime the system reaches global homochirality.

D. One-dimensional model of homochirality and the correlation function

In Sec. III C we saw that chiral molecules produced through autocatalytic processes in a spatial model stay at least locally homochiral even in the presence of diffusion, when autocatalysis is the dominant production mechanism. In other words, the noise-induced mechanism for homochirality is robust with respect to diffusion. But does the system stay globally homochiral? To answer this question, let us examine the continuous limit of Eq. (43). In the continuum limit, the noise term ξ_i (a side effect of diffusion on a discrete lattice) can be neglected. What is left of Eq. (43) in the continuous form can be written as

$$\frac{\partial \omega}{\partial t} = -\frac{2k_n\, k_d}{n\, k_a}\omega(t,\vec{x}) + \mathcal{D}\,\nabla^2\omega + \sqrt{\frac{2k_d}{n}(1-\omega^2)}\,\eta(t,\vec{x}), \tag{59}$$

where the Gaussian noise $\eta(t,\vec{x})$ is defined by its moments

$$\langle \eta(t,\vec{x})\eta(t',\vec{x}')\rangle = \delta(t-t')\,\delta(\vec{x}-\vec{x}') \tag{60}$$

and

$$\langle \eta(t,\vec{x})\rangle = 0, \tag{61}$$

and the diffusion coefficient $\mathcal{D} = \delta\, V^{2/D}$. After a change of variable (not shown here) Eq. (59) can be converted to a special case of what Korolev *et al.* [54] call "stochastic Fisher-Kolmogorov-Petrovsky-Piscounov equation [55,56] with additional terms describing mutation". We follow Ref. [54] to derive an equation for the time evolution of the two-point correlation function defined as

$$\phi(t,\vec{x}_1,\vec{x}_2) = \langle \omega(t,\vec{x}_1)\omega(t,\vec{x}_2)\rangle. \tag{62}$$

The correlation function $\phi(t,\vec{x}_1,\vec{x}_2)$ is a function of two stochastic variables $\omega(t,\vec{x}_1)$ and $\omega(t,\vec{x}_2)$, and its time derivative can be calculated using Itō's lemma from Eq. (59). The result has a beautiful closure property, where the right-hand side can be written in terms of ϕ:

$$\begin{aligned}\frac{\partial}{\partial t}\phi(t,\vec{x}_1,\vec{x}_2) = &-\frac{4k_nk_d}{nk_a}\phi(t,\vec{x}_1,\vec{x}_2)\\ &+\frac{2k_d}{n}(1-\phi(t,\vec{x}_1,\vec{x}_1))\,\delta(\vec{x}_1-\vec{x}_2)\\ &+\mathcal{D}\big(\nabla^2_{\vec{x}_1}+\nabla^2_{\vec{x}_2}\big)\phi(t,\vec{x}_1,\vec{x}_2).\end{aligned} \tag{63}$$

The two-point correlation function, $\phi(t,\vec{x}_1,\vec{x}_2)$, in Eq. (63) depends only on t and $\vec{x} = \vec{x}_1 - \vec{x}_2$ for spatially homogeneous initial conditions. With this simplification we have

$$\begin{aligned}\frac{\partial}{\partial t}\phi(t,\vec{x}) = 2\mathcal{D}\,\nabla^2\phi(t,\vec{x}) - \frac{2k_d}{n}[\phi(t,\vec{x})-1]\delta(\vec{x})\\ -\frac{4k_nk_d}{nk_a}\phi(t,\vec{x}).\end{aligned} \tag{64}$$

In one dimension, the steady-state solution of Eq. (64) can be obtained by setting the right-hand side equal to zero, and for $\phi(x) = \phi(\infty,x)$, we have

$$2\mathcal{D}\frac{\partial^2}{\partial x^2}\phi(x) - \frac{2k_d}{n}[\phi(x)-1]\delta(x) - \frac{4k_nk_d}{nk_a}\phi(x) = 0, \tag{65}$$

with the solution

$$\phi(x) = \frac{e^{-\sqrt{\frac{2k_nk_d}{n\mathcal{D}k_a}}|x|}}{1+\sqrt{\frac{8n\mathcal{D}k_n}{k_ak_d}}}. \tag{66}$$

The expected value of ω^2 is given by $\phi(0)$, and $\phi(x)$ exponentially decays from this value with the length scale

$$\zeta = \sqrt{\frac{n\mathcal{D}k_a}{2k_nk_d}}. \tag{67}$$

Therefore this length scale ζ defines a correlation length. This correlation length diverges as k_n approaches zero, indicating that in the pure autocatalytic limit of this model, at steady state, the entire space synchronizes its choice of homochirality to the same uniformly homochiral state. Figure 5 shows the result of simulation of reactions (42) in one dimension with $M = 100$ patches at the limit $k_n \to 0$. The simulation is initialized with a uniformly racemic state. The homochiral islands of D and L form very quickly at the beginning of the simulation and compete until the entire space becomes uniformly homochiral.

Here is an interesting fact about this spatial extension: Let us define the correlation volume $\mathcal{V} = (2\zeta)^D$ (this is the volume of the correlated cube from $-\zeta$ to ζ on each dimension), where the dimension $D = 1$ in this case. In terms of the correlation length and the correlation volume, the two-point correlation function is given by

$$\phi(x) = \frac{e^{-\left|\frac{x}{\zeta}\right|}}{1+2\frac{k_n\mathcal{V}}{k_a}} = \frac{e^{-\left|\frac{x}{\zeta}\right|}}{1+2\bar{\alpha}}. \tag{68}$$

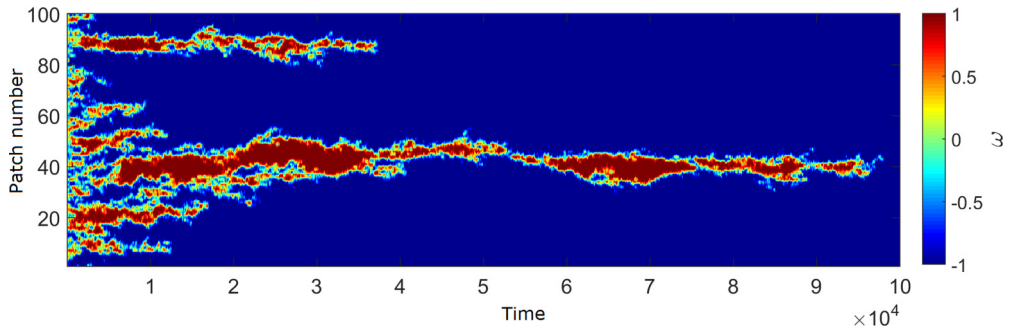

FIG. 5. Gillespie simulation of scheme reaction (42) for a one-dimensional system of $M = 100$ patches, starting from racemic state and ending with all the patches in the same homochiral state $\omega = -1$. Simulation parameters: $N = 1000$, $k_a = k_d = 1$, $\delta = 10^{-3}$, and $k_n = 0$.

The new $\bar{\alpha} = k_n \mathcal{V}/k_a$ is the α from the well-mixed case defined in Eq. (29) with the volume substituted by the correlation volume, $V = \mathcal{V}$. The expected value of ω^2 at each point is given by

$$\phi(0) = \frac{1}{1+2\bar{\alpha}}, \tag{69}$$

which is exactly the same if calculated from Eq. (29):

$$\begin{aligned}\langle \omega^2 \rangle &= \int_{-1}^{1} \omega^2 P(\omega)\, d\omega \\ &= \frac{\Gamma\left(\alpha+\frac{1}{2}\right)}{\sqrt{\pi}\Gamma(\alpha)} \int_{-1}^{1} \omega^2 (1-\omega^2)^{\alpha-1} d\omega = \frac{1}{1+2\alpha}.\end{aligned} \tag{70}$$

This shows that there is a correlation volume around every point in space in which the system behaves as though it is a well-mixed system with that volume.

IV. SPECULATIVE REMARKS AND FUTURE DIRECTIONS

We have proposed a mechanism for the initial symmetry breaking of the first self-replicating chiral molecules that only relies on minimal assumptions that are inseparable from the origin of life, namely a nonequilibrium chemical system involving self-replication and decay. We have also established the spatial stability of this mechanism and its robustness with respect to diffusion in a simple one dimensional system. But there is more to the problem of homochirality. Here are a few examples of important questions left unanswered in the field.

The field clearly lacks a theoretical framework to explore how the homochirality of different chemical compounds are related: Why do all amino acids have the same handedness, and what is the relationship between the chirality of, e.g., sugars and amino acids. Did different organic molecules become homochiral in a particular order, or was there an interdependence between homochirality of different types of molecules forcing the homochirality to occur at the same time for all the organic compounds involved in the origin of life?

Once the initial symmetry breaks in one of the species, the system is no longer symmetric. The homochiral solution of one of the chiral compounds interacts differently with other chiral molecules, and in theory, could select for a particular enantiomer of other molecules.[7] Despite this fact, there are interesting problems that are worth investigating related this synchronization, the solution to which depends on the mechanism of origin of life.

We are long way from having all the details on the origin of life to be able to find the order through which various chemical compounds have become homochiral. The answer to this question relies on the answer to a different question: when did homochirality arise with respect to the origin of life? Were first self-replicators very simple chemical compounds, or were they chemical complexes made of several molecules?

If one believes the RNA world picture of the origin of life [57], perhaps homochirality started with homochirality of sugars, and when the first ribosomes were formed, they could force their choice of chirality on the amino acids. In contrast, if the first self-replicating complexes involved both amino acids and nucleic acids [58], or if self-replication first manifested in multistep processes involving both peptides and nucleic acids (as it is the case in modern organisms), the problem becomes more complex. In such scenarios, one should develop more complex models involving several chiral species with their replications coupled. The interaction network of various chiral molecules involved in self-replication can be arbitrarily complex, but one can get away with just modeling a cyclic autocatalytic reaction set of N species. That is because all statistical properties of complex autocatalytic reaction networks can be computed by reducing the network to cycles, and the entire behavior is determined by one dominant cycle [59].

We speculate that even in the second scenario, where the first self-replicators involved both amino acids and nucleic acids, the presence of a ribosome-like molecule could be responsible for coordination of the chirality of different types of amino acids. It is important to note that the ability of polypeptides to form α helices and β sheets relies on the uniform homochirality across all amino acids [60].

Another potential future direction in this paradigm is to model the evolution toward homochirality. We have shown that when the efficiency of self-replication is higher than a

[7] This is how modern organisms maintain their homochirality; all the enzymes are asymmetric and their asymmetric shape can restrict their interactions with other chiral molecules to a particular enantiomer, selecting one of the two symmetric reactions.

threshold (that is when the majority of self-replicators are produced through self-replication, and not spontaneously), the population transitions to homochirality. We also argued that even if the system starts with inefficient self-replicators, over time, they evolve to become more efficient at self-replication and therefore transition to homochirality. A potential model to show this process can be constructed by allowing the rate of the self-replication reaction to perform a random walk through each generation (modeling stochastic changes in self-replication processes) and show that in such population, the population average of the parameter α that describes the efficiency of self-replication increases over time with no extra assumptions. This model is mathematically challenging since the reaction rates depend on the particular random walk trajectories that ancestral lineage of each self-replicator has taken, but the numerical simulations should be tractable.

From the experimental side, we would love to see a confirmation of the noise-induced symmetry-breaking mechanism in an externally driven system with recycling to clarify the time scales associated with this phenomenon in a real experimental setting. Such experiments could be performed using template replicating RNA (similar to those used in Ref. [16]). These experiments need to be performed in nonequilibrium open flow systems with recycling, where reactants are constantly added and products removed from experiment.

Finally, in this work, we have shown that homochirality (if emerged through the mechanism proposed) does not depend on specific chemical details of origin of life; it relies only on the defining characteristics of life, i.e., nonequilibrium self-replication and decay. This property of our model has a distinct prediction with important implications in the field of astrobiology, that is, if chiral life were to be found outside of our planet, it has to be homochiral, while its choice chirality for different molecules need not agree with similar terrestrial molecules. When or if appropriate technology is developed to detect homochirality from a distance, homochirality can be used as a more robust biosignature in search for extraterrestrial life.

V. CONCLUSION

In conclusion, a racemic population of self-replicating chiral molecules far from equilibrium, even in the absence of other nonlinearities that have previously been invoked, such as chiral inhibition, transitions to complete homochirality when the efficiency of self-replication exceeds a certain threshold. This transition occurs due to the drift of the chiral order parameter under the influence of the intrinsic stochasticity of the autocatalytic reactions. The functional form of the multiplicative intrinsic noise from autocatalysis directs this drift toward one of the homochiral states. Unlike some other mechanisms in the literature, this process does not require an initial enantiomeric excess. In our model, the homochiral states are not deterministic dynamical fixed points, but are instead stabilized by intrinsic noise. Moreover, in the spatial extension of our model, we have shown that diffusively coupled autocatalytic systems synchronize their final homochiral states, allowing a system solely driven by autocatalysis to reach global homochirality. We conclude that autocatalysis alone is a viable mechanism for homochirality, without the necessity of imposing chiral inhibition or other nonlinearities.

ACKNOWLEDGMENTS

We thank Elbert Branscomb for valuable discussions. This material is based upon work supported by the National Aeronautics and Space Administration through the NASA Astrobiology Institute under Cooperative Agreement No. NNA13AA91A, issued through the Science Mission Directorate.

APPENDIX A: DECOUPLING GAUSSIAN NOISE

Consider a set of coupled stochastic differential equations

$$\frac{d\vec{x}}{dt} = \vec{H}(\vec{x}) + \vec{\xi}(t), \tag{A1}$$

where ξ_i ($i \in \{1,\ldots,n\}$), the components of $\vec{\xi}(t)$, are zero mean Gaussian noise functions with correlation

$$\langle \xi_i(t)\xi_j(t')\rangle = B_{i,j}\delta(t-t'). \tag{A2}$$

We would like to rewrite Eq. (A1) in terms of some set of independent Gaussian white noise functions $\eta_i(t)$ ($i \in \{1,\ldots,m\}$ for some m) with the correlation

$$\langle \eta_i(t)\eta_j(t')\rangle = \delta_{i,j}\delta(t-t'). \tag{A3}$$

If we can find an $n \times m$ matrix $\mathbf{G}$ such that $\mathbf{B} = \mathbf{G}\mathbf{G}^{\mathsf{T}}$, then it is straightforward to show that $\vec{\xi}(t) = \mathbf{G}\vec{\eta}(t)$:

$$\begin{aligned}\langle \xi_i(t)\xi_j(t')\rangle &= \left\langle \sum_k G_{i,k}\eta_k(t) \sum_l G_{j,l}\eta_l(t') \right\rangle \\ &= \sum_{k,l} G_{i,k}G_{j,l}\langle \eta_k(t)\eta_l(t')\rangle \\ &= \sum_{k,l} G_{i,k}G_{j,l}\delta_{k,l}\delta(t-t') \\ &= \sum_k G_{i,k}G^{\mathsf{T}}_{k,j}\delta(t-t') = B_{i,j}\delta(t-t'). \end{aligned} \tag{A4}$$

Now Eq. (A1) in terms of $\vec{\eta}(t)$ is given by

$$\frac{d\vec{x}}{dt} = \vec{H}(\vec{x}) + \mathbf{G}\vec{\eta}(t). \tag{A5}$$

This decomposition is not unique and multiple choices for $\mathbf{G}$ exist [44]. Perhaps the simplest choice is given by the $n \times n$ matrix $\mathbf{G} = \mathbf{B}^{1/2}$. Note that matrix $\mathbf{B}$ is symmetric positive definite and therefore, is diagonalizable and has a well-defined real symmetric square root. Hence $\mathbf{G}\mathbf{G}^{\mathsf{T}} = \mathbf{G}\mathbf{G} = \mathbf{G}^2 = \mathbf{B}$.

The Fokker-Planck equations derived from a set of reactions or species interactions have a $\mathbf{B}$ matrix with the particular structure (see, e.g., Sec. II B)

$$\mathbf{B} = \sum_{i=1}^{m} T_i\, \vec{s}_i \otimes \vec{s}_i, \tag{A6}$$

where $\vec{s}_i$ is the ith row of an $m \times n$ stoichiometry matrix $\mathbf{S}$. For such $\mathbf{B}$, there is a particular choice of matrix $\mathbf{G}$ whose matrix elements have simpler analytic expressions compared to the

square root choice:

$$G_{i,j} = \sqrt{T_j}\, S_{j,i}. \tag{A7}$$

It is straightforward to show that $\mathbf{G}\mathbf{G}^{\mathsf{T}} = \mathbf{B}$:

$$\begin{aligned}(\mathbf{G}\mathbf{G}^{\mathsf{T}})_{i,j} &= \sum_k G_{i,k}\, G_{j,k} \\ &= \sum_k \sqrt{T_k} S_{k,i} \sqrt{T_k} S_{k,j} \\ &= \left(\sum_k T_k\, \vec{s}_k \otimes \vec{s}_k \right)_{i,j} = B_{i,j}. \end{aligned} \tag{A8}$$

The number of columns, m, of matrix $\mathbf{G}$ from this method is the same as the number of reactions from which the Fokker-Planck equation is derived. In the special case, where the stoichiometry matrix $\mathbf{S}$ has rows that are multiples of each other, there are simpler choices of $\mathbf{G}$ obtained by reducing the rows of $\mathbf{S}$ before calculating $\mathbf{G}$ through the following procedure: Suppose, for example $\vec{s}_j = a\,\vec{s}_i$. Then, we simply remove the row j of $\mathbf{S}$ (and the corresponding T_j) and replace T_i by $T_i + a^2\, T_j$. The reason that this row reduction works is that the reduced matrix $\mathbf{S}$ and corresponding T define the same matrix $\mathbf{B}$ as before:

$$\begin{aligned}\mathbf{B} &= \sum_{k=1}^{m} T_k\, \vec{s}_k \otimes \vec{s}_k \\ &= \cdots + T_i\, \vec{s}_i \otimes \vec{s}_i + \cdots + T_j\, \vec{s}_j \otimes \vec{s}_j + \cdots \\ &= \cdots + T_i\, \vec{s}_i \otimes \vec{s}_i + \cdots + a^2\, T_j\, \vec{s}_i \otimes \vec{s}_i + \cdots \\ &= \sum_{k \neq i,j} T_k\, \vec{s}_k \otimes \vec{s}_k + (T_i + a^2\, T_j) \vec{s}_i \otimes \vec{s}_i. \end{aligned} \tag{A9}$$

APPENDIX B: MEAN SWITCHING TIME

Let us define the dimensionless time τ as

$$\tau = \frac{2tk_d}{N}. \tag{B1}$$

In terms of τ, Eq. (27) becomes

$$\frac{d\omega}{d\tau} = -\alpha\omega + \sqrt{(1-\omega^2)}\eta(\tau), \tag{B2}$$

with

$$\langle \eta(\tau)\eta(\tau') \rangle = \delta(\tau - \tau'). \tag{B3}$$

We follow Ref. [41] to calculate the mean switching time from one homochiral state $\omega = -1$ the other $\omega = 1$. We impose an absorbing boundary condition on the final state for the probability density of ω:

$$P(1,\tau) = 0 \tag{B4}$$

with the initial condition

$$P(\omega,0) = \delta(\omega + 1). \tag{B5}$$

To find the probability density of the switching time, $\rho(\tau)$, we use the fact that the probability of switching happening after the time τ is the same as probability of that the system has not been absorbed by the boundary before time τ:

$$\int_\tau^\infty \rho(\tau')d\tau' = \int_{-1}^{1} P(\omega,\tau)d\omega. \tag{B6}$$

The switching time probability density function can be calculated by differentiating both sides with respect to τ. Let us define $G(\tau',\omega;\tau)$ as the probability that the system has not been absorbed by the boundary at time τ given that it started at some point ω at time τ'. This probability satisfies the backward Kolmogorov equation

$$\frac{\partial G}{\partial \tau'} - \alpha\,\omega \frac{\partial G}{\partial \omega} + \frac{1}{2}(1-\omega^2)\frac{\partial^2 G}{\partial \omega^2} = 0, \tag{B7}$$

with the terminal condition

$$G(\tau,\omega;\tau) = 1, \tag{B8}$$

and the absorbing boundary condition

$$G(\tau',1;\tau) = 0. \tag{B9}$$

In terms of G, the probability density, ρ, of the absorbing time given the initial condition (τ',ω) is given by

$$\rho(\tau|\tau',\omega) = -\frac{\partial}{\partial \tau} G(\tau',\omega;\tau). \tag{B10}$$

We define the mean absorbing time, given the initial condition (τ',ω) by

$$\langle \tau \rangle_{\tau',\omega} = \int_{\tau'}^{\infty} \tau \rho(\tau|\tau',\omega) d\tau. \tag{B11}$$

Assuming G decays sufficiently fast at $\tau \to \infty$ limit, we have

$$\begin{aligned}\langle \tau \rangle_{\tau',\omega} &= \int_0^\infty \tau \rho(\tau|\tau',\omega)\, d\tau = -\int_{\tau'}^{\infty} \tau \frac{\partial}{\partial \tau} G(\tau',\omega;\tau)\, d\tau \\ &= -\tau G(\tau',\omega;\tau)\big|_{\tau'}^{\infty} + \int_{\tau'}^{\infty} G(\tau',\omega;\tau)\, d\tau \\ &= \tau' + \int_{\tau'}^{\infty} G(\tau',\omega;\tau)\, d\tau \end{aligned} \tag{B12}$$

Now, we can integrate Eq. (B7) to obtain a differential equation for $\langle \tau \rangle_{\tau',\omega}$:

$$1 - \alpha\,\omega \frac{\partial}{\partial \omega}\langle \tau \rangle_{\tau',\omega} + \frac{1}{2}(1-\omega^2)\frac{\partial^2}{\partial \omega^2}\langle \tau \rangle_{\tau',\omega} = 0, \tag{B13}$$

where we have used the fact that the probability G only depends on the time difference $\tau - \tau'$ (Markovian property) and therefore

$$\begin{aligned}\frac{\partial}{\partial \tau'}\langle \tau \rangle_{\tau',\omega} &= 1 + \frac{\partial}{\partial \tau'} \int_{\tau'}^{\infty} G(\tau',\omega;\tau)\, d\tau \\ &= 1 + \int_{\tau'}^{\infty} \frac{\partial}{\partial \tau'} G(\tau',\omega;\tau)\, d\tau - G(\tau',\omega;\tau') \\ &= 1 - \int_{\tau'}^{\infty} \frac{\partial}{\partial \tau} G(\tau',\omega;\tau)\, d\tau - G(\tau',\omega;\tau') \\ &= 1 - G(\tau',\omega;\infty) = 1. \end{aligned} \tag{B14}$$

There are two boundary conditions, the first one at $\omega = 1$:

$$\langle \tau \rangle_{\tau',1} = \tau'. \tag{B15}$$

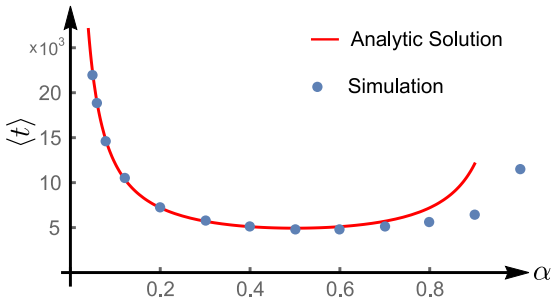

FIG. 6. Mean switching time, $\langle t\rangle$, from one homochiral state to the other as a function of α. Analytical result (solid red line) from Eq. (B19) compared with the Gillespie simulation results (blue points). The analytical expression is valid for small α where the system is homochiral. For α close to 1 or greater (where the system is expected to stay racemic), to accurately predict the mean switching time, one needs to keep track of higher order term (in $1/N$) in the corresponding Fokker-Planck equation. Simulation parameters: $k_d = 1$, $k_a = 1$, $k_n = 1$, $N = 1000$, and $V = \alpha$.

The second one at $\omega = -1$ is a tricky one. We know that the dynamics has a naturally reflecting boundary at $\omega = -1$, because of the way the ratio ω is defined confines it to $[-1,1]$. Given this reflecting boundary condition, a stochastic trajectory staring at $\omega = -1$ can only move in one direction, with the velocity $-\alpha\omega = \alpha$. Therefore,

$$\frac{\partial}{\partial\omega}\langle\tau\rangle_{\tau',\omega} = -\frac{1}{\alpha}. \tag{B16}$$

The solution for Eq. (B13) with these boundary conditions is given by

$$\begin{aligned}\langle\tau\rangle_{\tau',\omega} = \tau' - \omega^2\,{}_3F_2\left(1,1,\alpha+\frac{1}{2};\frac{3}{2},2;\omega^2\right)\\ + \frac{\pi\cot(\pi\alpha)}{1-2\alpha} + \frac{H_{-\alpha}+\log(4)}{1-2\alpha}\\ - \frac{\sqrt{\pi}\omega\Gamma(\alpha)\,{}_2F_1\left(\frac{1}{2},\alpha;\frac{3}{2};\omega^2\right)}{\Gamma\left(\alpha+\frac{1}{2}\right)},\end{aligned} \tag{B17}$$

where ${}_pF_q$ are hypergeometric functions, $H_{-\alpha}$ is generalized harmonic number evaluated at $-\alpha$, and Γ are gamma functions.

Mean switching time $\langle\tau\rangle = \langle\tau\rangle_{0,-1}$ is given by

$$\langle\tau\rangle = \frac{2\pi\cot(\pi\alpha)}{1-2\alpha}. \tag{B18}$$

Going back to the dimensionful variables, the mean switching time $\langle t\rangle$ is given by

$$\langle t\rangle = \frac{N\pi\cot(\pi\alpha)}{k_d(1-2\alpha)}. \tag{B19}$$

The mean switching time approaches infinity for small α, large N, or small k_d. Figure 6 shows that this analytic result agrees with the Gillespie simulation of reactions (9) when the system is in the homochiral regime $\alpha \ll 1$. To find the mean switching time for the parameter regime $\alpha > 1$ (where the system is expected to stay racemic), we need to keep track of higher order terms in the Fokker-Planck approximation when deriving Eq. (27) [41].

[1] K. Vetsigian, C. Woese, and N. Goldenfeld, Proc. Natl. Acad. Sci USA **103**, 10696 (2006).
[2] L. Pasteur, *Recherches sur les relations qui peuvent exister entre la forme cristalline, la composition chimique et les sens de la polarisation rotatoire* (Impr. Bachelier, 1848).
[3] J. L. Bada, Nature (London) **374**, 594 (1995).
[4] J. Bailey, Origins Life Evol. Biosph. **31**, 167 (2001).
[5] Y. Yamagata, J. Theor. Biol. **11**, 495 (1966).
[6] W. A. Bonner, Chirality **12**, 114 (2000).
[7] S. Pizzarello and J. Cronin, Nature (London) **394**, 236 (1998).
[8] F. C. Frank, Biochim. Biophys. Acta **11**, 459 (1953).
[9] K. Soai, T. Shibata, H. Morioka, and K. Choji, Nature (London) **378**, 767 (1995).
[10] M. Gleiser and S. I. Walker, Orig. Life Evol. Biosph. **38**, 293 (2008).
[11] D. K. Kondepudi and G. W. Nelson, Phys. Rev. Lett. **50**, 1023 (1983).
[12] R. Plasson, H. Bersini, and A. Commeyras, Proc. Natl. Acad. Sci. USA **101**, 16733 (2004).
[13] Y. Saito and H. Hyuga, J. Phys. Soc. Jpn. **73**, 33 (2004).
[14] P. Sandars, Orig. Life Evol. Biosph. **33**, 575 (2003).
[15] Y. Saito and H. Hyuga, Rev. Mod. Phys. **85**, 603 (2013).
[16] J. T. Sczepanski and G. F. Joyce, Nature (London) **515**, 440 (2014).
[17] F. Jafarpour, T. Biancalani, and N. Goldenfeld, Phys. Rev. Lett. **115**, 158101 (2015).
[18] J. H. vant Hoff, Arch. Néerlandaises Sci. exactes naturelles **9**, 445 (1874).
[19] J. A. Le Bel, Bull. Soc. Chim. France **22**, 337 (1874).
[20] G. Moss, Pure Appl. Chem. **68**, 2193 (1996).
[21] P. M. Kim, X. Duan, A. S. Huang, C. Y. Liu, G.-l. Ming, H. Song, and S. H. Snyder, Proc. Natl. Acad. Sci. USA **107**, 3175 (2010).
[22] H. Kleinkauf and H. von Döhren, *EJB Reviews 1990* (Springer, New York, 1990), pp. 151–165.
[23] F. Cava, H. Lam, M. A. de Pedro, and M. K. Waldor, Cell. Mol. Life Sci. **68**, 817 (2011).
[24] M. H. Engel and S. Macko, Nature (London) **389**, 265 (1997).
[25] J. R. Cronin and S. Pizzarello, Science **275**, 951 (1997).
[26] T.-D. Lee and C.-N. Yang, Phys. Rev. **104**, 254 (1956).
[27] C. Wu, E. Ambler, R. Hayward, D. Hoppes, and R. Hudson, Phys. Rev. **105**, 1413 (1957).
[28] G. Joyce, G. Visser, C. Van Boeckel, J. Van Boom, L. Orgel, and J. Van Westrenen, Nature (London) **310**, 602 (1984).
[29] M. Gleiser, B. J. Nelson, and S. I. Walker, Orig. Life Evol. Biosph. **42**, 333 (2012).
[30] A. Brandenburg, H. J. Lehto, and K. M. Lehto, Astrobiology **7**, 725 (2007).
[31] G. Lente, Symmetry **2**, 767 (2010).
[32] R. Shibata, Y. Saito, and H. Hyuga, Phys. Rev. E **74**, 026117 (2006).
[33] R. Plasson, D. K. Kondepudi, and K. Asakura, J. Phys. Chem. B **110**, 8481 (2006).

[34] D. Hochberg and M.-P. Zorzano, Chem. Phys. Lett. **431**, 185 (2006).
[35] D. Hochberg and M. P. Zorzano, Phys. Rev. E **76**, 021109 (2007).
[36] G. Lente, J. Phys. Chem. A **108**, 9475 (2004).
[37] C. W. Gardiner, *Handbook of Stochastic Methods for Physics, Chemistry and the Natural Sciences*, 4th ed. (Springer, New York, 2009).
[38] Y. Togashi and K. Kaneko, Phys. Rev. Lett. **86**, 2459 (2001).
[39] M. N. Artyomov, J. Das, M. Kardar, and A. K. Chakraborty, Proc. Natl. Acad. Sci. USA **104**, 18958 (2007).
[40] D. I. Russell and R. A. Blythe, Phys. Rev. Lett. **106**, 165702 (2011).
[41] T. Biancalani, L. Dyson, and A. J. McKane, Phys. Rev. Lett. **112**, 038101 (2014).
[42] N. G. van Kampen, *Stochastic Processes in Physics and Chemistry*, 3rd ed. (Elsevier Science, Amsterdam, 2007).
[43] D. T. Gillespie, J. Phys. Chem. **81**, 2340 (1977).
[44] A. J. McKane, T. Biancalani, and T. Rogers, Bull. Math. Biol. **76**, 895 (2014).
[45] T. Biancalani, L. Dyson, and A. J. McKane, J. Stat. Mech. (2015) P01013.
[46] D. G. Blackmond, Angew. Chem., Int. Ed. **48**, 2648 (2009).
[47] R. Wegscheider, Monatsh. Chem./Chem. Month. **32**, 849 (1911).
[48] J. R. Knowles, Annu. Rev. Biochem. **49**, 877 (1980).
[49] R. Plasson, J. Phys. Chem. B **112**, 9550 (2008).
[50] J. L. Bada, J. Am. Chem. Soc. **94**, 1371 (1972).
[51] J. L. Bada, X. S. Wang, H. N. Poinar, S. Pääbo, and G. O. Poinar, Geochim. Cosmochim. Acta **58**, 3131 (1994).
[52] W. Martin, J. Baross, D. Kelley, and M. J. Russell, Nat. Rev. Microbiol. **6**, 805 (2008).
[53] A. J. McKane and T. J. Newman, Phys. Rev. E **70**, 041902 (2004).
[54] K. S. Korolev, M. Avlund, O. Hallatschek, and D. R. Nelson, Rev. Mod. Phys. **82**, 1691 (2010).
[55] R. A. Fisher, Ann. Eugenics **7**, 355 (1937).
[56] A. N. Kolmogorov, I. Petrovsky, and N. Piskunov, Moscow Univ. Math. Bull **1**, 1 (1937).
[57] W. Gilbert, Nature (London) **319**, 618 (1986).
[58] K. E. Nelson, M. Levy, and S. L. Miller, Proc. Natl. Acad. Sci. USA **97**, 3868 (2000).
[59] S. Iyer-Biswas, G. E. Crooks, N. F. Scherer, and A. R. Dinner, Phys. Rev. Lett. **113**, 028101 (2014).
[60] A. Kumar, V. Ramakrishnan, R. Ranbhor, K. Patel, and S. Durani, J. Phys. Chem. B **113**, 16435 (2009).